Electronic Supplementary Material (ESI) for Physical Chemistry Chemical Physics.

Electronic Supplementary Information (ESI)

to

Properties of perhalogenated {*closo*-B_{10}} and {*closo*-B_{11}} multiply charged anions and a critical comparison with {*closo*-B_{12}} in the gas and the condensed phase

Jonas Warneke[1*], Szymon Z. Konieczka[2], Gao-Lei Hou[1], Edoardo Aprà[3], Christoph Kerpen[2], Fabian Keppner[2], Thomas C. Schäfer[2], Michael Deckert[2], Zheng Yang[1], Eric J. Bylaska[3], Grant E. Johnson[1], Julia Laskin[4], Sotiris S. Xantheas[5,6], Xue-Bin Wang[1], Maik Finze[2*]

[1] Physical Sciences Division, Pacific Northwest National Laboratory, 902 Battelle Boulevard, P.O. Box 999, MSIN K8-88, WA, 99352, USA, contact: E-mail: Jonas.Warneke@pnnl.gov

[2] Julius-Maximilians-Universität Würzburg, Institute for Inorganic Chemistry, Institute for Sustainable Chemistry & Catalysis with Boron (ICB), Am Hubland, 97074 Würzburg, Germany E-mail: maik.finze@uni-wuerzburg.de

[3] Environmental Molecular Sciences Laboratory, Pacific Northwest National Laboratory, P. O. Box 999, Richland, WA 99352, USA

[4] Department of Chemistry, Purdue University, West Lafayette, IN 47907, USA

[5] Advanced Computing, Mathematics and Data Division, Pacific Northwest National Laboratory, 902 Battelle Boulevard, P.O. Box 999, MS K1-83, WA, 99352, USA

[6] Department of Chemistry, University of Washington, Seattle, WA, 98195, USA

SI1. Interpretation of PES spectra.

The experimental vertical detachment energy (VDE) of all a) [*closo*-B_nX_n]$^{2-}$ dianions and b) [*closo*-B_nX_n•$N(C_4H_9)$]$^-$ singly negatively charged ion pairs was determined from the maximum of the first resolved spectral band, corresponding to the transition from the initial ground state of the dianion or ion pair to the final electronic ground state of the a) singly charged anion [*closo*-B_nX_n]$^-$ or b) neutral [*closo*-B_nX_n•$N(C_4H_9)$], respectively, with the highest Franck-Condon factor between the initial and final states. It is worth noting that for closed-shell dianions/or anions with high symmetry, photodetachment will lead to an open shell final system, which is often subject to Jahn-Teller distortion. Consequently, degenerate molecular orbitals in the initial precursor molecule split under the lower symmetry, giving rising to visible fine structures (not due to vibrational progression) within otherwise one spectral feature. For example, dodecaborate dianions [*closo*-$B_{12}X_{12}$]$^{2-}$ (X = Cl, Br) have a quadruply degenerate HOMO. Photodetachment of one electron from this HOMO of [*closo*-$B_{12}X_{12}$]$^{2-}$ leads to the first spectral band that has a fine structure composed of three maxima, because the initial quadruply degenerate HOMO splits into three different energy levels in low symmetric [$B_{12}X_{12}$]$^{\bullet-}$. As such, VDE should be measured from the true first peak maximum (sometimes exhibited as a shoulder in the band). For spectra like the ones in this work, in which no vibrational progression is resolved, the adiabatic detachment energy (ADE) is estimated from the onset of the first spectral band. In addition, density of states (DOS) spectra based on theoretically generalized Koopmans' theorem (GKT)[1] can be used to further analyse the experimental spectrum as previous studies have shown. GKT is a useful way to qualitatively interpret the PES spectra.[2-3] The simulated DOS spectra are obtained by setting the HOMO transition of the anion as the first experimental VDE, and then uniformly shifting transitions from lower lying orbitals. (Note that the concept of DOS has been widely used in solid state physics in the context of electronic band structures. Here we do not describe electronic bands but rather distinct orbital energy levels.) Therefore, the absence of spectral features in a certain energy range often correlates to the absence of occupied MOs in the corresponding energy range.

SI2. Comparison of VDEs, ADEs and density of states (DOS) predicted by DFT and Hartree-Fock

Table S1 compares the calculated values for ADE and VDE of B_{10}- and B_{11}-clusters for HF and DFT/PBE0 level of theory with the experimentally measured values. In a previous investigation on B12 clusters, we found that PBE0 systematically underestimates the experimental values, while HF slightly overestimates them.[4] In agreement with this, we found that HF VDE values were systematically higher than PBE0 values also for B_{10} and B_{11} clusters, however the values for the clusters with chlorine ligands were slightly underestimated, while the values for iodinated compounds were slightly overestimated. The trend for ADEs is similar, but the HF values for the chlorinated compounds were significantly too low.

Table S1. Comparison of experimental (yellow) and computationally determined VDEs and ADEs in eV of investigated compounds.

Dianion	VDE (HF)	VDE (PBE0)	VDE (PES)	ADE (HF)	ADE (PBE0)	ADE (PES)
[*closo*-$B_{10}Cl_{10}]^{2-}$	1.70	1.68	1.80	1.29	1.42	1.55
[*closo*-$B_{11}Cl_{11}]^{2-}$	1.75	1.64	1.80	1.37	1.40	1.55
[*closo*-$B_{10}Br_{10}]^{2-}$	2.14	1.97	2.15	1.78	1.75	1.90
[*closo*-$B_{11}Br_{11}]^{2-}$	2.17	1.93	2.10	1.80	1.72	1.90
[*closo*-$B_{10}I_{10}]^{2-}$	2.52	2.17	2.50	2.22	2.03	2.15
[*closo*-$B_{11}I_{11}]^{2-}$	2.50	2.15	2.40	2.18	2.01	2.15

Note that DFT orbitals have been shown in the past to accurately fit the features of PES spectra. Figure S1 exemplifies on the basis of DOS representations and PES spectra of the brominated 10-, 11-, and 12-vertex *closo*-borate anions that this is not the case for the anions studied in this contribution and that Hartree-Fock orbitals should be used to describe DOS.

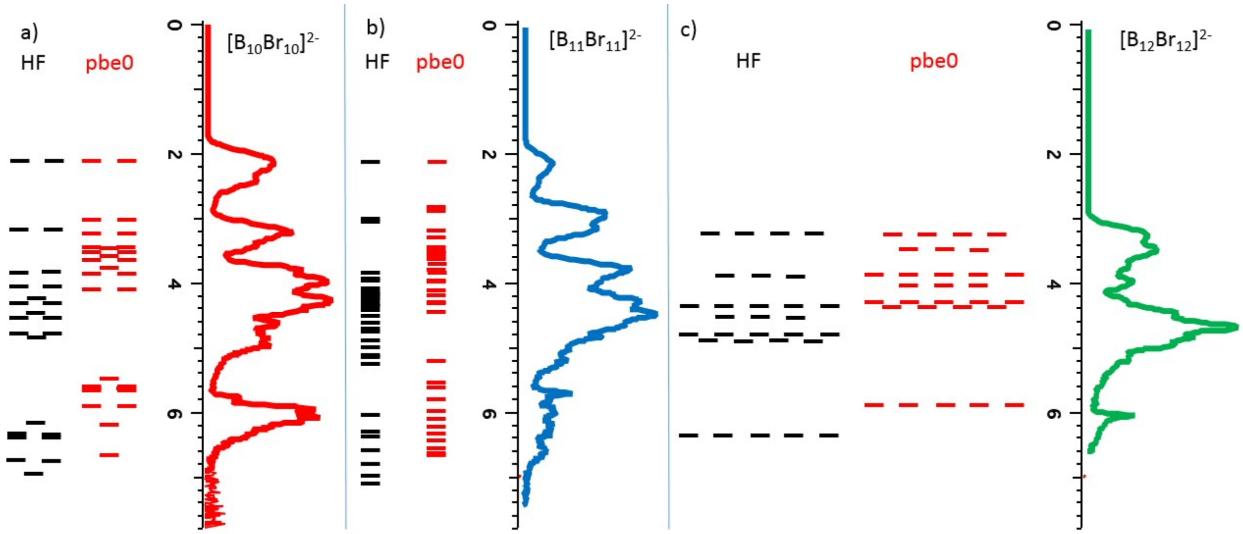

Figure S1. Comparison between computational predicted DOS by Hartree-Fock and DFT/PBE0 in comparison with measured PES spectra on the example of investigated brominated *closo*-borates. The HOMO energy was shifted in all cases to the experimental VDE.

SI3. Hatree-Fock orbital diagrams

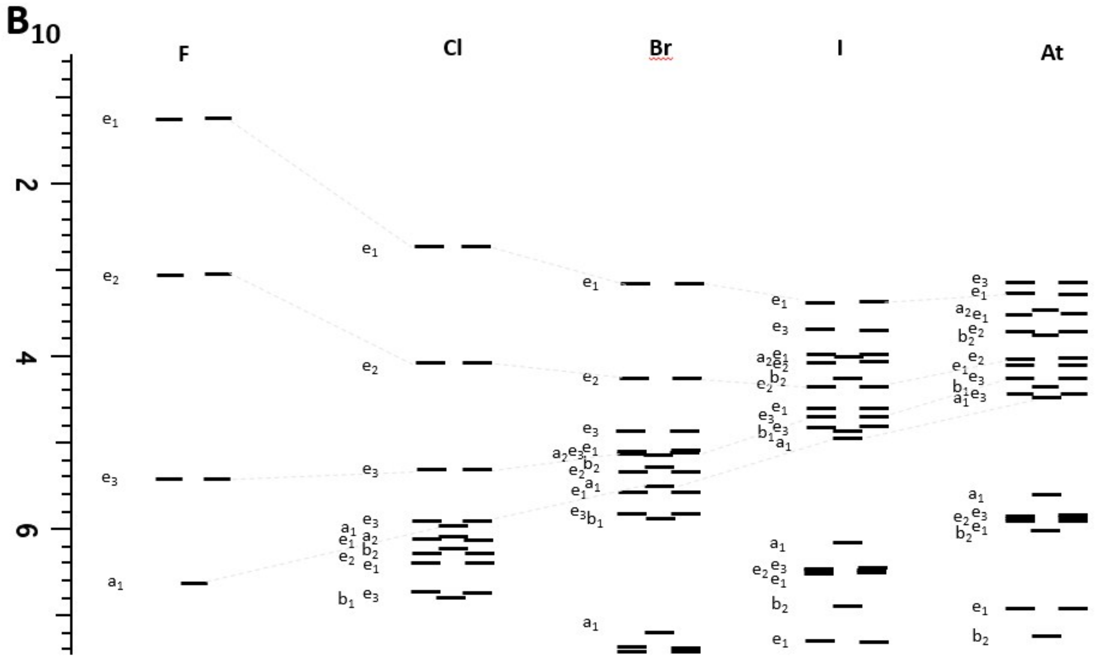

Figure S2. Orbital energy and symmetry for [*closo*-$B_{10}X_{10}$]$^{2-}$ (X = F, Cl, Br, I, At)

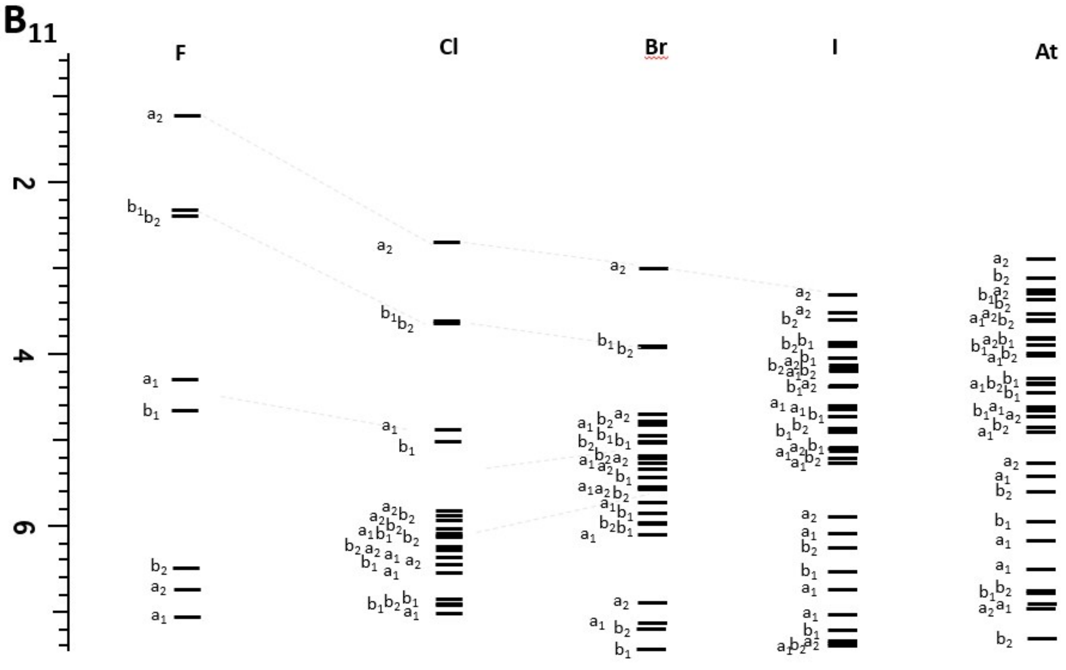

Figure S3. Orbital energy and symmetry for [*closo*-$B_{11}X_{11}$]$^{2-}$ (X = F, Cl, Br, I, At).

SI4. Natural population analysis

Table S2. List of summed NPA values for the boron core (B_{total}) and the halogen shell (X_{total}) and the ranges of values for the individual atoms B and *X* (*X* = F, Cl, Br, I).

	B_{total}	X_{total}	value range B	value range *X*
[*closo*-$B_{10}F_{10}$]$^{2-}$	2.8	-4.8	+0.15/+0.31	-0.48
[*closo*-$B_{10}Cl_{10}$]$^{2-}$	-0.28	-1.72	-0.19/+0.01	-0.17
[*closo*-$B_{10}Br_{10}$]$^{2-}$	-1.07	-0.93	-0.27/-0.07	-0.09
[*closo*-$B_{10}I_{10}$]$^{2-}$	-2.09	0.09	-0.36/-0.17	+0.01
[*closo*-$B_{11}F_{11}$]$^{2-}$	3.22	-5.22	+0.27/+0.50	-0.47/-0.49
[*closo*-$B_{11}Cl_{11}$]$^{2-}$	-0.23	-1.77	-0.23/+0.24	-0.16
[*closo*-$B_{11}Br_{11}$]$^{2-}$	-1.15	-0.85	-0.31/+0.15	-0,07/-0.08
[*closo*-$B_{11}I_{11}$]$^{2-}$	-2.32	0.32	-0.41/+0.02	+0.02/+0.06
[*closo*-$B_{12}F_{12}$]$^{2-}$	3.57	-5.57	+0.30	-0.46
[*closo*-$B_{12}Cl_{12}$]$^{2-}$	-0.22	-1.78	-0,02	-0,15
[*closo*-$B_{12}Br_{12}$]$^{2-}$	-0.94	-1.06	-0,08	-0,09
[*closo*-$B_{12}I_{12}$]$^{2-}$	-2.51	0.51	-0,21	+0.04

SI5. PES spectra of the ion pair ([*closo*-$B_n$$Cl_n$]+TBA])$^-$

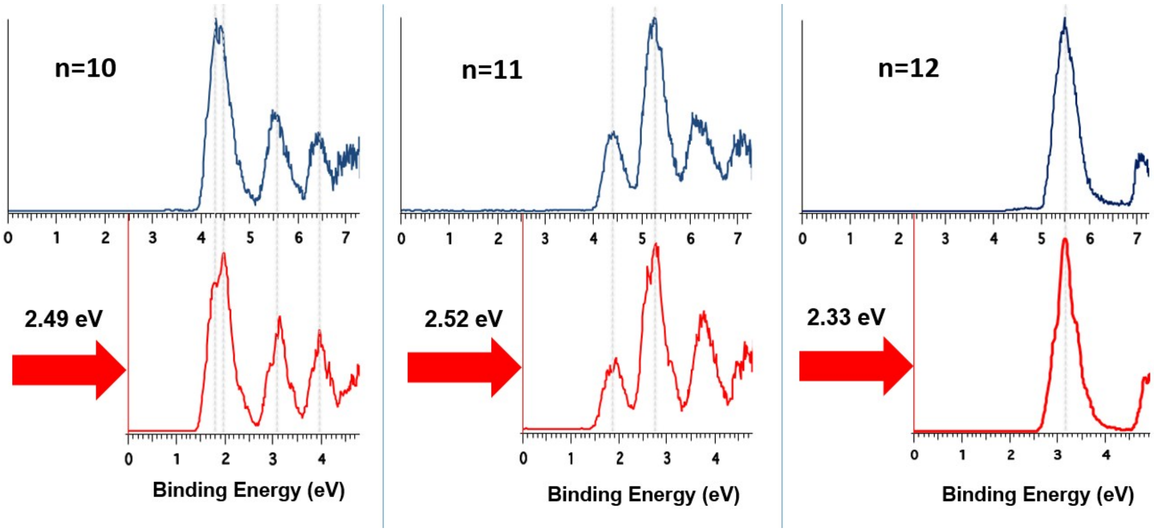

Figure S4. Comparison of ([*closo*-$B_n$$Cl_n$]+TBA)$^–$ (blue) and [*closo*-$B_n$$Cl_n$]$^{2–}$ (red) PES spectra (157 nm). The shift in the electron binding energy is related to the interaction strength with the counter cation. The uncertainty for these values is estimated to be 0.05 eV.

SI6. Different binding sites for tetramethylammonium counter ion to the [*closo*-$B_{11}Cl_{11}$]$^{2-}$ dianion

We are using tetramethylammonium as counterion to simplify the calculations. Experiments have been performed with [Bu_4N]$^+$. To evidence the legitimacy of this simplification we performed VDE calculations on the optimized [$B_{12}Cl_{12}$+$(CH_3)_4N$]$^-$ and [$B_{12}Cl_{12}$+Bu_4N]$^-$. The obtained VDEs were 5.12 and 5.08eV. The influence of of the bulkiness of the alkyl chains can therefore be considered to be in the range of 0.05 eV.

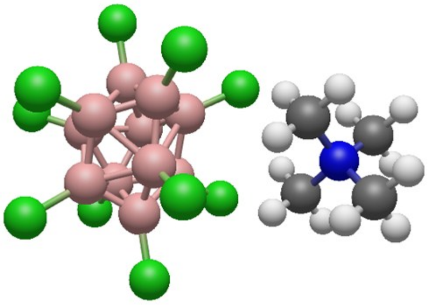

Figure S5. Coordination site with the lowest energy for the model ion pair composed of [Me_4N]$^+$ and [*closo*-$B_{11}Cl_{11}$]$^{2-}$. Total energy: -5548,711 a.u., VDE: 4.17 eV, VDE shift with respect to the bare dianion [$B_{11}Cl_{11}$]$^{2-}$: 2.56eV (compare to Figure S4).

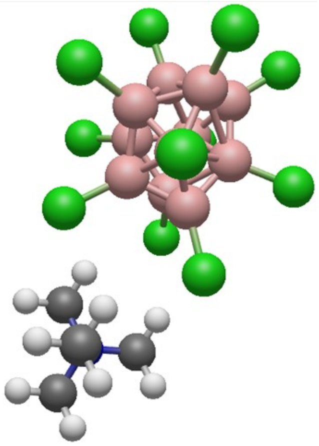

Figure S6. A selected coordination site for the ammonium ion different from the lowest energy structure. Total energy: –5548,706 Ha, VDE: 4.05 eV, VDE shift with respect to the bare dianion [*closo*-$B_{11}Cl_{11}$]$^{2-}$: 2.43 eV (compare to Figure S4).

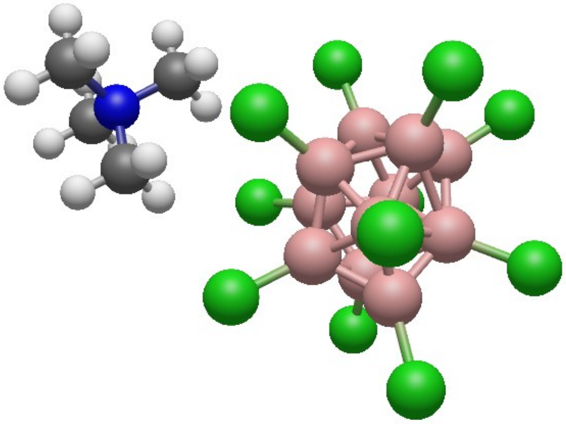

Figure S7. Highest symmetrical structure found for the ion pair of $[Me_4N]^+$ with [*closo*-$B_{11}Cl_{11}]^{2-}$ (C_{2v}), which is different from the lowest energy structure. Total energy: –5548.556 a.u., VDE: 4.08 V, VDE shift with respect to the bare dianion [*closo*-$B_{11}Cl_{11}]^{2-}$: 2.46 eV (compare to Figure S4).

SI7: Detailed explanation of the ions observed in the mass spectra shown in Figure 5b)

Ions that originate from cation fragmentation are marked with a brown background in Figure 5. The respective ion pair fragments by loss of neutral tributylamine and leaves behind a butyl cation on the boron cluster:

$$[closo\text{-}B_{12}X_{12}N(C_4H_9)_4]^- \rightarrow [closo\text{-}B_{12}X_{12}(C_4H_9)]^- + N(C_4H_9)_3 \qquad (1)$$

This butyl cation fragments by loss of butene to yield a protonated dodecaborate:

$$[closo\text{-}B_{12}X_{12}(C_4H_9)]^- \rightarrow [closo\text{-}B_{12}X_{12}H]^- + C_4H_9 \qquad (2)$$

Protonated dodecaborates act as anionic gas phase Lewis acids and add water from the background of the mass spectrometer:

$$[closo\text{-}B_{12}X_{12}H]^- + H_2O \rightarrow [closo\text{-}B_{12}X_{12}H_3O]^- \qquad (3)$$

The products of these three reactions account for the three brown peaks observed in the case of X = Br. For X = Cl, only peaks corresponding to (2) and (3) are visible, because (1) has been fragmented almost completely by secondary dissociation reactions. In the case of X = I, no peak corresponding to (3) is visible because the iodinated gas phase acid does not protonate water.[5]

SI8: Ion acetonitrile interaction

Structures were optimized with PBE0/def2-tzvppd

VDE ([*closo*-$B_{10}Cl_{10}$]$^{2-}$): 1.66 eV

VDE ([*closo*-$B_{10}Cl_{10}(CH_3CN)$]$^{2-}$): 1.98 eV Stabilization: 0.32 eV

VDE ([*closo*-$B_{10}I_{10}$]$^{2-}$): 2.16 eV

VDE ([*closo*-$B_{10}I_{10}(CH_3CN)$]$^{2-}$): 2.40 eV Stabilization: 0.24 eV

VDE ([*closo*-$B_{12}Cl_{12}$]$^{2-}$): 2.74 eV

VDE ([*closo*-$B_{12}Cl_{12}(CH_3CN)$]$^{2-}$): 3.02 eV Stabilization: 0.28 eV

VDE ([*closo*-$B_{12}I_{12}$]$^{2-}$): 2.37 eV

VDE ([*closo*-$B_{12}I_{12}(CH_3CN)$]$^{2-}$): 2.59 eV Stabilization: 0.22 eV

SI9: Cyclic voltammetry

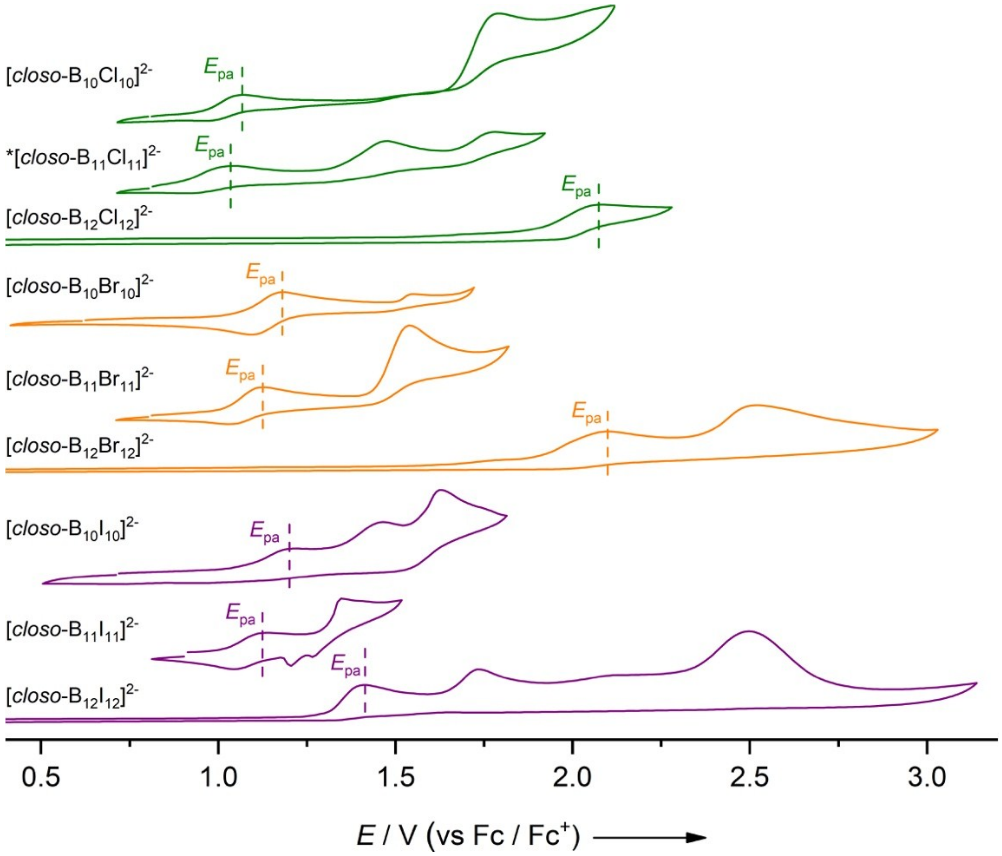

Figure S8. Cyclic voltammograms of [nBu$_4$N]$_2$[*closo*-$B_{10}X_{10}$], [nBu$_4$N]$_2$[*closo*-$B_{11}X_{11}$], and [nBu$_4$N]$_2$[*closo*-$B_{12}X_{12}$] (X = Cl, Br, I) in acetonitrile ($c = 1 \cdot 10^{-3}$ mol L^{-1}; scan rate v = 100 mV s^{-1}, glassy-carbon working electrode, Pt counter electrode, and reference electrode with 0.01 mol L^{-1} $AgNO_3$ and 0.1 mol L^{-1} [nBu$_4$N][PF$_6$] in acetonitrile; *[nBu$_4$N]$_2$[*closo*-$B_{11}Cl_{11}$] contains 33% of [nBu$_4$N]$_2$[*closo*-$B_{10}Cl_{10}$], compare Table S3).

Table S3. Anodic and cathodic peak potentials of $[n\mathrm{Bu_4N}]_2[\textit{closo}\text{-}\mathrm{B}_{11}X_{11}]$ (X = Cl, Br, I) in acetonitrile.

Compound	E_{pa1} [V][a]	E_{pc1} [V][a]	$E_{1/2}$ [V][a]	ΔE_1 [mV][a]	E_{pa2} [V][a]
$[\textit{closo}\text{-}\mathrm{B}_{11}\mathrm{Cl}_{11}]^{2-}$ [b]	1.04[c]	0.92[c]	0.98[c]	121[c]	1.46
$[\mathrm{BzEt_3N}]^+$ salt in $\mathit{CH_2Cl_2}$ 6	*1.1*[d]	–	–	–	–
$[\textit{closo}\text{-}\mathrm{B}_{11}\mathrm{Br}_{11}]^{2-}$	1.12	1.04	1.08	85	1.53
$[\mathrm{BzEt_3N}]^+$ salt in $\mathit{CH_2Cl_2}$ 6	–	–	*0.97*	–	*1.18 in $\mathit{CH_3CN}$*
$[\textit{closo}\text{-}\mathrm{B}_{11}\mathrm{I}_{11}]^{2-}$	1.14	1.05	1.09	85	[e]
$[\mathrm{BzEt_3N}]^+$ salt in $\mathit{CH_3CN}$ 6	*1.3*[f]	–	–	–	–

[a] Versus Fc/Fc$^+$; scan rate: v = 100 mV s^{-1}, glassy carbon working electrode, Pt counter electrode, and reference electrode with 0.01 mol L^{-1} $\mathrm{AgNO_3}$ and $[n\mathrm{Bu_4N}][\mathrm{PF_6}]$ 0.1 mol L^{-1} in acetonitrile. [b] $^*[n\mathrm{Bu_4N}]_2[\textit{closo}\text{-}\mathrm{B}_{11}\mathrm{Cl}_{11}]$, contains 33% of $[n\mathrm{Bu_4N}]_2[\textit{closo}\text{-}\mathrm{B}_{10}\mathrm{Cl}_{10}]$. The additional anodic peak observed in the cyclic voltammogram in Figure S8 at 1.79 V is assigned to E_{pa2} of $[n\mathrm{Bu_4N}]_2[\textit{closo}\text{-}\mathrm{B}_{10}\mathrm{Cl}_{10}]$ as listed in Table S2. [c] The anodic and cathodic peak overlaps with the respective peaks of $[n\mathrm{Bu_4N}]_2[\textit{closo}\text{-}\mathrm{B}_{10}\mathrm{Cl}_{10}]$ listed in Table S2, which may lead to a slight error of the potentials given. [d] The oxidation peak is immediately followed by a second one.6 [e] A further assignment of the relative weak anodic and cathodic peaks shown in Figure S8 is omitted. [f] The oxidation is followed by a number of follow-up oxidation peaks.6

Table S4. Anodic and cathodic peak potentials of $[n\mathrm{Bu}_4\mathrm{N}]_2[closo\text{-}\mathrm{B}_{12}X_{12}]$ (X = Cl, Br, I) in acetonitrile (this work) and data taken from the literature.

Anion	E_{pa1} [V][a]	E_{pc1} [V][a]	$E_{1/2}$ [V][a]	ΔE_1 [mV][a]	E_{pa2} [V][a]
$[closo\text{-}\mathrm{B}_{12}\mathrm{Cl}_{12}]^{2-}$	2.08 (2.17[7])	–	–	–	2.96
Na⁺ salt in SO₂ at –59 °C [7]	*2.15*	*2.07*	*2.11*	*80*	*2.67* *(–49 °C)*
$[closo\text{-}\mathrm{B}_{12}\mathrm{Br}_{12}]^{2-}$	2.10	1.94	2.02	151	2.52
Na⁺ salt in SO₂ at –58 °C [7]	*2.31*	*2.23*	*2.27*	*80*	*2.67*
$[closo\text{-}\mathrm{B}_{12}\mathrm{I}_{12}]^{2-}$ [b]	1.41	1.30	1.36	110	2.1
Na⁺ salt in SO₂ at –56 °C [7]	*2.1*	–	–	–	*2.2–2.3*

[a] Versus Fc/Fc$^+$; scan rate: v = 100 mV s^{-1}, glassy carbon working electrode, Pt counter electrode, and reference electrode with 0.01 mol L^{-1} $\mathrm{AgNO_3}$ and $[n\mathrm{Bu}_4\mathrm{N}][\mathrm{PF}_6]$ 0.1 mol L^{-1} in acetonitrile. [b] The assignment of the peaks to the $[closo\text{-}\mathrm{B}_{12}\mathrm{I}_{12}]^{2-}$ ion was aided by a comparison to the cyclic voltammogram of $[n\mathrm{Bu}_4\mathrm{N}]\mathrm{I}$ shown in Figure S9.

Comments on the cyclic voltammetry study on $[n\mathrm{Bu}_4\mathrm{N}]_2[closo\text{-}\mathrm{B}_{12}\mathrm{I}_{12}]$ in $\mathrm{CH_3CN}$:

Figure S9 shows the CVs of purified $[n\mathrm{Bu}_4\mathrm{N}]_2[closo\text{-}\mathrm{B}_{12}\mathrm{I}_{12}]$, crude $[n\mathrm{Bu}_4\mathrm{N}]_2[closo\text{-}\mathrm{B}_{12}\mathrm{I}_{12}]$ isolated from the reaction mixture, and neat $[n\mathrm{Bu}_4\mathrm{N}]\mathrm{I}$. After purification of $[n\mathrm{Bu}_4\mathrm{N}]_2[closo\text{-}\mathrm{B}_{12}\mathrm{I}_{12}]$ less events are present in the CV and the curve is almost flat in the range of –1 to 1 V. The oxidation events in the CV of pure $[n\mathrm{Bu}_4\mathrm{N}]_2[closo\text{-}\mathrm{B}_{12}\mathrm{I}_{12}]$ at 1.73 and 2.50 V (Table S5) can be assigned to follow-up oxidations of an iodine-containing compound released from $[closo\text{-}\mathrm{B}_{12}\mathrm{I}_{12}]^{2-}$ after its oxidation, since these oxidation events agree to the ones found in the CV of $[n\mathrm{Bu}_4\mathrm{N}]\mathrm{I}$. So, the first oxidation peak potential of $[closo\text{-}\mathrm{B}_{12}\mathrm{I}_{12}]^{2-}$ is assigned to 1.41 V and further oxidation of the radical ion $[closo\text{-}\mathrm{B}_{12}\mathrm{I}_{12}]^{\cdot-}$ is assigned to the event at 2.1 V because these events are missing in the CV curve of $[n\mathrm{Bu}_4\mathrm{N}]\mathrm{I}$.

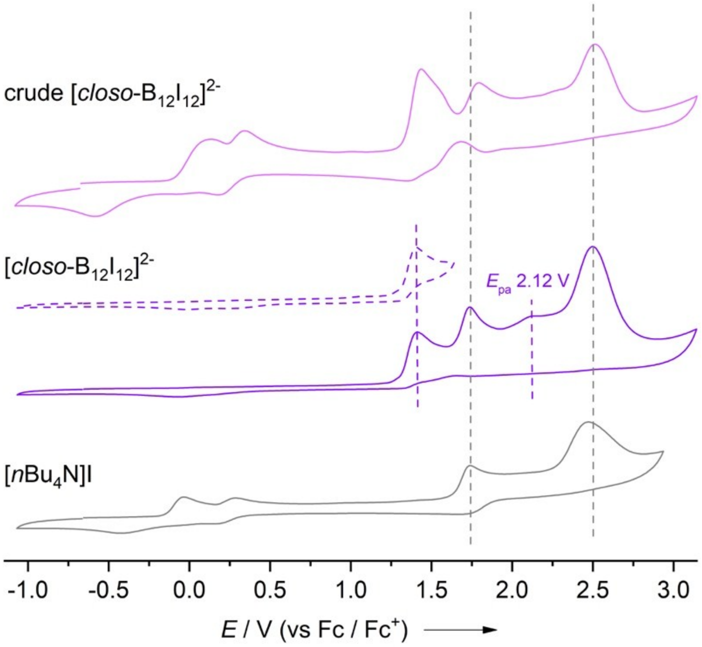

Figure S9. Cyclic voltammograms of neat $[nBu_4N]_2[closo\text{-}B_{12}I_{12}]$ (purple), crude $[nBu_4N]_2[closo\text{-}B_{12}I_{12}]$ (magenta), and $[nBu_4N]I$ (grey) in acetonitrile (c = $1\cdot10^{-3}$ mol L^{-1}; scan rate v = 100 mV s^{-1}, glassy-carbon working electrode, Pt counter electrode, and reference electrode with 0.01 mol L^{-1} $AgNO_3$ and 0.1 mol L^{-1} $[nBu_4N][PF_6]$ in acetonitrile).

Table S5. Selected anodic peak potentials observed in the CVs of $[nBu_4N]I$ and $[nBu_4N]_2[closo\text{-}B_{12}I_{12}]$.

Anion	E_{pa} [V][a]	E_{pa} [V][a]	E_{pa} [V][a]	E_{pa} [V][a]
$[closo\text{-}B_{12}I_{12}]^{2-}$	1.41	1.73	2.1	2.50
I^-	–	1.74	–	2.48

[a] Versus Fc/Fc$^+$; scan rate: v = 100 mV s^{-1}, glassy-carbon working electrode, Pt counter electrode, and reference electrode with 0.01 mol L^{-1} $AgNO_3$ and $[nBu_4N][PF_6]$ 0.1 mol L^{-1} in acetonitrile.

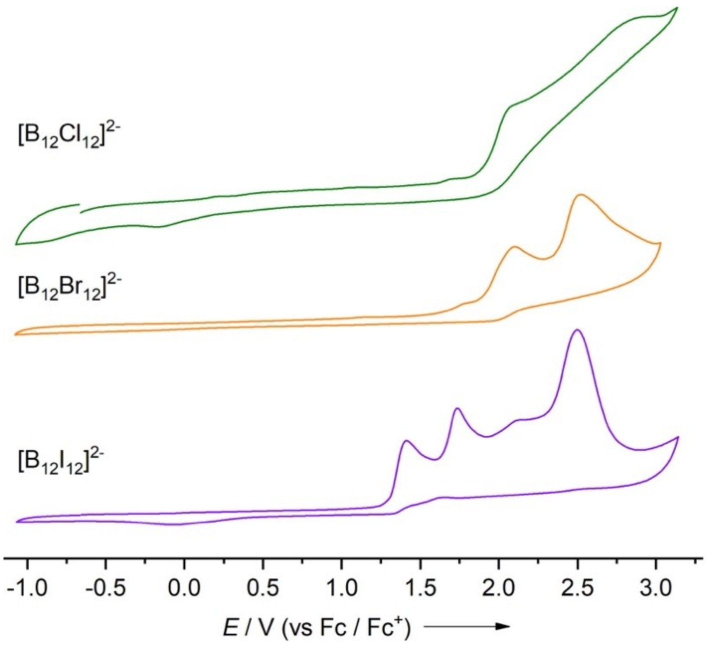

Figure S10. Cyclic voltammograms of $[n\mathrm{Bu}_4\mathrm{N}]_2[closo\text{-}\mathrm{B}_{12}X_{12}]$ (X = Cl, Br, I) in acetonitrile in the region of ca. –1 to 3 V ($c = 1\cdot10^{-3}$ mol L^{-1}; scan rate v = 100 mV s^{-1}, glassy-carbon working electrode, Pt counter electrode, and reference electrode with 0.01 mol L^{-1} $AgNO_3$ and 0.1 mol L^{-1} $[n\mathrm{Bu}_4\mathrm{N}][\mathrm{PF}_6]$ in acetonitrile).

Table S6. Summary of the first anodic peak potential assigned to the oxidation process of $[n\text{Bu}_4\text{N}]_2[closo\text{-B}_n X_n]$ (X = Cl, Br, I; n = 10–12) in acetonitrile.

Anion	E_{pa1} [V][a]
$[closo\text{-B}_{10}\text{Cl}_{10}]^{2-}$	1.07
$[closo\text{-B}_{11}\text{Cl}_{11}]^{2-}$	1.04
$[closo\text{-B}_{12}\text{Cl}_{12}]^{2-}$	2.08
$[closo\text{-B}_{10}\text{Br}_{10}]^{2-}$	1.18
$[closo\text{-B}_{11}\text{Br}_{11}]^{2-}$	1.12
$[closo\text{-B}_{12}\text{Br}_{12}]^{2-}$	2.10
$[closo\text{-B}_{10}\text{I}_{10}]^{2-}$	1.21
$[closo\text{-B}_{11}\text{I}_{11}]^{2-}$	1.14
$[closo\text{-B}_{12}\text{I}_{12}]^{2-}$	1.41

[a] Versus Fc/Fc$^+$; scan rate: v = 100 mV s^{-1}, glassy carbon working electrode, Pt counter electrode, and reference electrode with 0.01 mol L^{-1} AgNO_3 and $[n\text{Bu}_4\text{N}][\text{PF}_6]$ 0.1 mol L^{-1} in acetonitrile.

SI10: Results of Molecular Dynamic simulations

Two independent AIMD simulations in the canonical ensemble at 300 K have been carried out for [*closo*-$B_{10}Cl_{10}$]$^{2-}$ and [*closo*-$B_{12}Cl_{12}$]$^{2-}$ clusters dissolved in 56 acetonitrile molecules (C_2H_3N, SMILES: CC#N) in a periodic unit cell. In these simulations, no counter ions were present, and the -2 charge of the clusters was neutralized by a uniform background charge of opposite sign. The AIMD simulations were based on gradient-corrected (PBE) density functional theory and the Car-Parrinello molecular dynamics (CPMD) algorithm as implemented in the NWChem computational chemistry code. A plane wave basis cutoff of 100 Ry and Γ point sampling were used to expand DFT wave functions. Simple cubic cells with L = 16.935 Å and L = 17.256 Å were used for the [*closo*-$B_{10}Cl_{10}$]$^{2-}$ + 56 C_2H_3N and [*closo*-$B_{12}Cl_{12}$]$^{2-}$ + 56 C_2H_3N simulations, respectively. The interactions between valence electrons and the atom centers were approximated using generalized norm-conserving Hamann pseudopotentials for H, B, C, and N; and a norm-conserving Troullier–Martin pseudopotential, which contained a semi-core correction. The pseudopotentials were modified into a separable form as suggested by Kleinman and Bylander. For gradient corrected calculations, the NWPW module automatically generates pseudopotentials using the specified exchange correlation functional. The original pseudopotential parameterization suggested by Hamann was slightly softened by increasing the core radii: H: r_{cs} = 0.8 a.u., r_{cp} = 0.8 a.u.; B: r_{cs} = 1.1 a.u., r_{cp} = 0.9 a.u., and r_{cd} = 1.1 a.u.; C: r_{cs} = 0.80 a.u., r_{cp} = 0.85 a.u., and r_{cd} = 0.85 a.u.; and N: r_{cs} = 0.7 a.u., r_{cp} = 0.7 a.u., and r_{cd} = 0.7 a.u.. The core radii for the Cl pseudopotential were chosen to be r_{cs} = 1.34 a.u., r_{cp} = 1.45 a.u., and r_{cd} = 1.45 a.u. The equations of motions in CPMD were integrated using position Verlet algorithm, with a time step 0.12 fs for a total of 35 ps and fictitious orbital mass of 750.0 au. All hydrogen atoms were replaced by deuterium to facilitate the integration. The simulation was carried out in a constant temperature canonical ensemble (300 K) using Nose-Hoover thermostats to control the temperatures of the ions and the 1-electron orbitals.

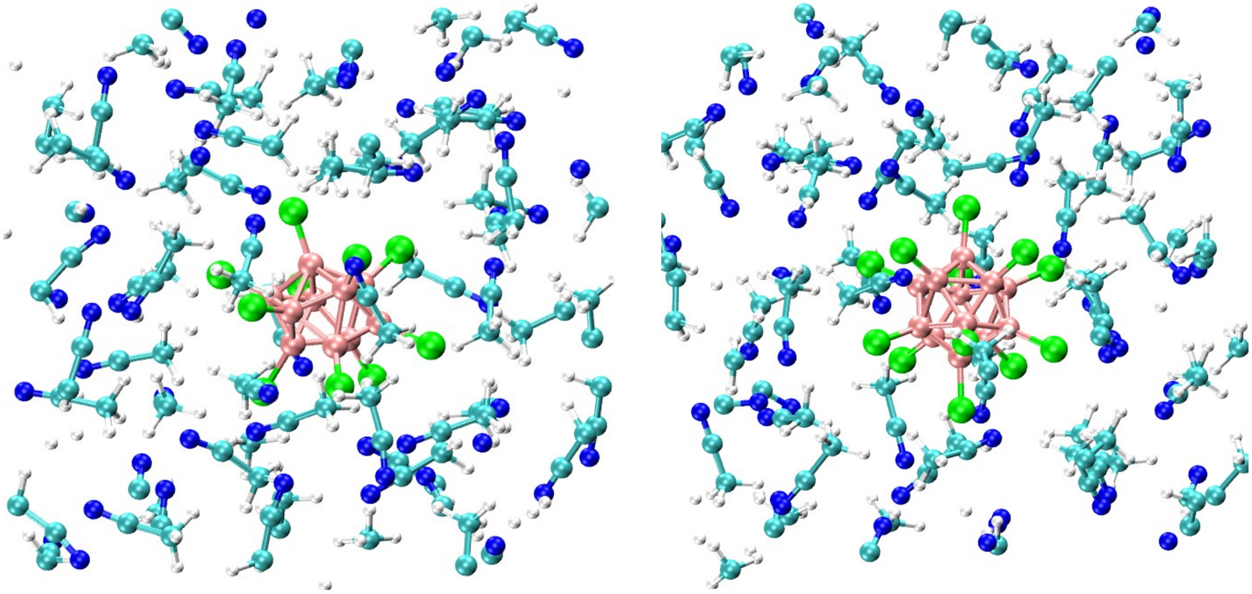

Figure S11. Image of [*closo*-$B_{10}Cl_{10}$]$^{2-}$ (left) and [*closo*-$B_{12}Cl_{12}$]$^{2-}$ (right) in acetonitrile.

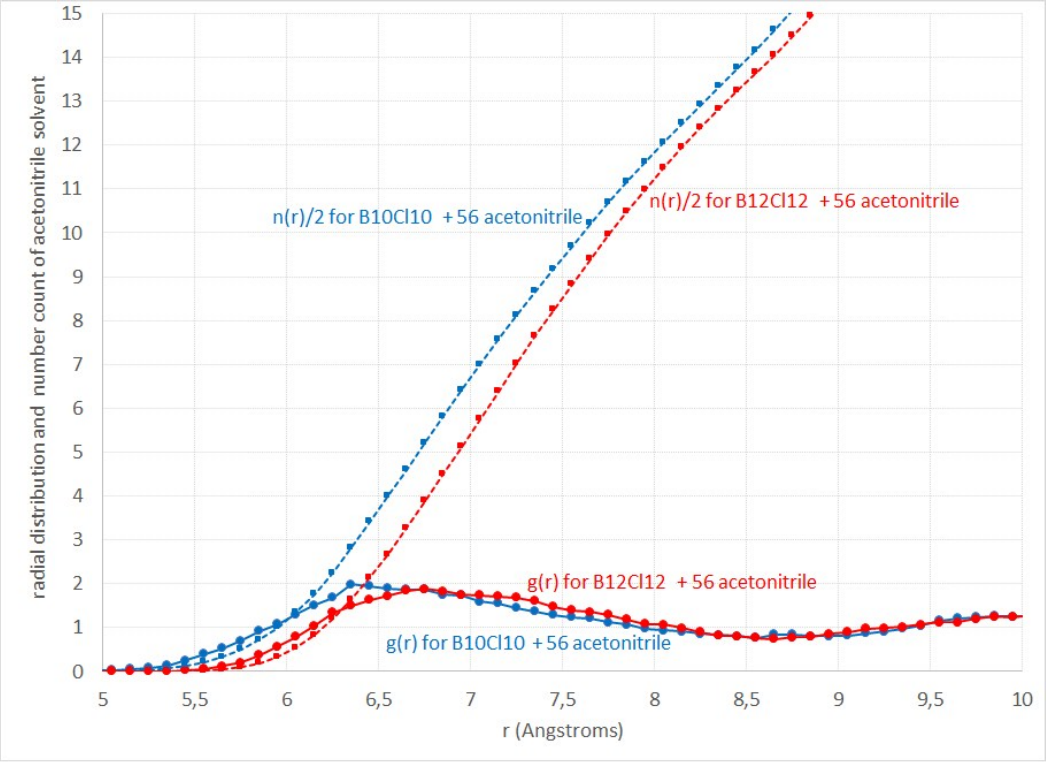

Figure S12. The radial distribution functions, g(r) and running coordination number functions, n(r) derived from AIMD simulations. The radial distribution functions were defined between the center of the [*closo*-$B_{10}Cl_{10}$]$^{2-}$ and [*closo*-$B_{12}Cl_{12}$]$^{2-}$ clusters and the location of the center carbon (CN group) in the acetonitrile molecules. These distributions show that the first shell is broad and flat. An integration up to the first minimum of g(r) results in the estimation of 28.33 acetonitrile molecules for the first solvation shell of [*closo*-$B_{10}Cl_{10}$]$^{2-}$ and 26.90 molecules in the first solvation shell of [*closo*-$B_{12}Cl_{12}$]$^{2-}$. The number of molecules in the first shell appears to be the same for both clusters, with the first shell slightly pushed out from the larger [*closo*-$B_{12}Cl_{12}$]$^{2-}$ cluster.

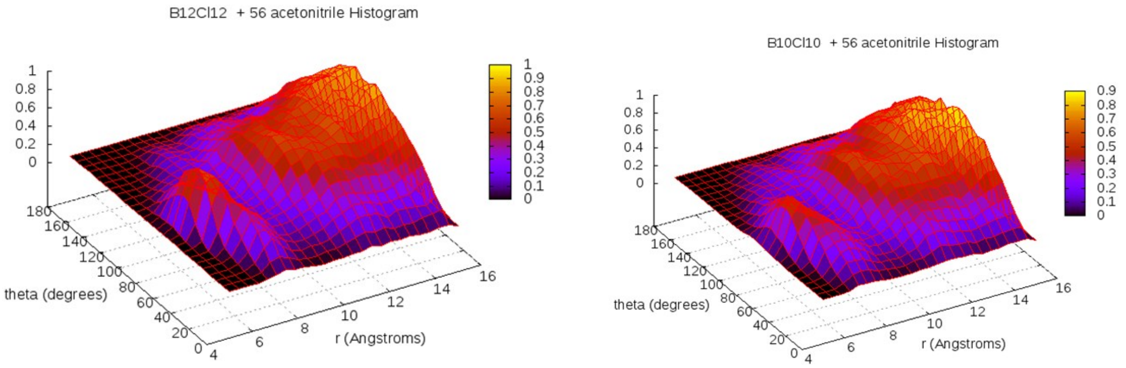

Figure S13. Two-dimensional histogram plots where the x axis is the radial distance and the y axis is the dipole angle, where the dipole angle is defined to be the angle between the vector between the center of the [*closo*-$B_{10}Cl_{10}$]$^{2-}$ and [*closo*-$B_{12}Cl_{12}$]$^{2-}$ clusters and the center of the acetonitrile molecules and the direction of the acetonitrile molecules. There is a slight preference in the orientation of the methyl groups of the acetonitrile molecules towards the clusters. These plots also show that there is very little difference between the first shell structure of the two clusters.

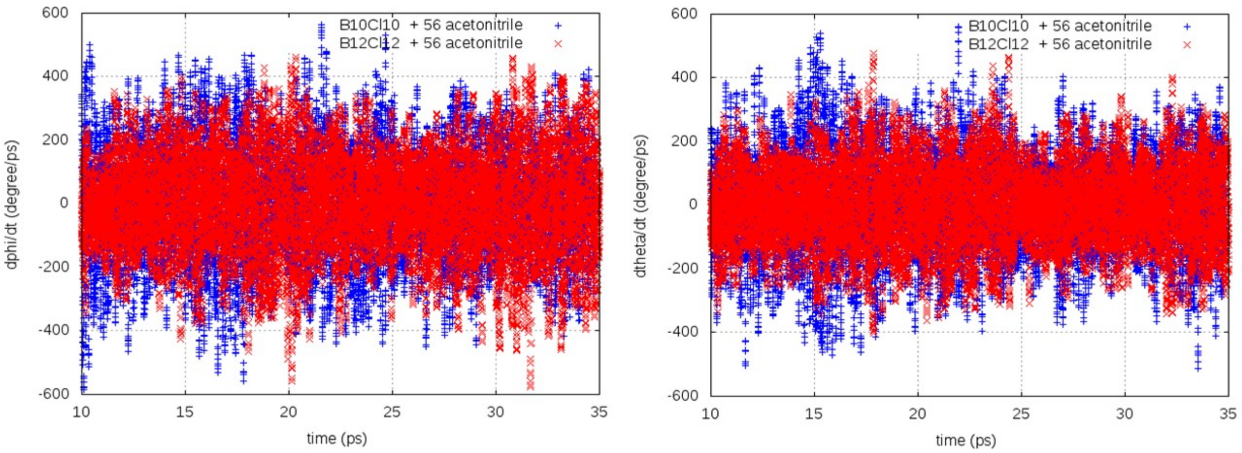

Figure S14. Plots of the instantaneous rotational velocities ($\dot{\phi}$,$\dot{\theta}$) of the [*closo*-$B_{10}Cl_{10}$]$^{2-}$ and [*closo*-$B_{12}Cl_{12}$]$^{2-}$ clusters. No discernable differences are seen between the distributions of these velocities for the two different cluster.

SI11: Synthesis and Analysis of Compounds

Analytical Instruments and Details

^{1}H, ^{11}B, and ^{13}C NMR spectra were recorded at 25 °C in CD_3CN on a Bruker Avance 500 or a Bruker Avance 400 spectrometer. NMR signals were referenced against TMS (^{1}H and ^{13}C; $\Xi(^{13}C)$ = 25.145020 MHz) and $BF_3 \cdot OEt_2$ in $CDCl_3$ ($\Xi(^{11}B)$ = 32.083974 MHz).[8] The ^{1}H and ^{13}C chemical shifts were calibrated against the residual solvent signal and the solvent signal, respectively (CD_2HCN: $\delta(^{1}H)$ = 1.94 ppm; CD_3CN: $\delta(^{13}C)$ = 118.26 and 1.32 ppm).[9] (–)-MALDI mass spectra were acquired with an Autoflex II LRF (Bruker Daltonics). Elemental analyses (C, H, N) were performed with a Euro EA3000 instrument (HEKA-Tech, Germany).

Chemicals

All standard chemicals (NCS = *N*-chlorosuccinimide, tetrabutylammonium hydroxide, bromine, iodine, iodine monochloride, potassium hydroxide, chlorine, and sodium sulfite) were obtained from commercial sources und used without further purification. Solvents (dichloromethane, water, acetonitrile, ethanol, methanol, and tetrachloroethane) were used without further purification, as well. $K_2[closo\text{-}B_{11}H_{11}]$ was synthesized according to a literature procedure.[10] The halogenated $[nBu_4N]_2[closo\text{-}B_{10}X_{10}]$[11] and $[nBu_4N]_2[closo\text{-}B_{12}X_{12}]$[11-12] (X = Cl, Br, I) were synthesized as described elsewhere. *tert*-Butyl hypochlorite was obtained via a known procedure.[13]

Syntheses

Preparation of $[nBu_4N]_2[closo\text{-}B_{11}H_{11}]$. $K_2[closo\text{-}B_{11}H_{11}]$ (2.24 g, 10.76 mmol) was dissolved in water (20 mL) and an aqueous solution of $[nBu_4N]OH$ (27.0 g, 40 wt%, 41.6 mmol) was added while stirring. The white precipitate was filtered off and washed with water (100 mL). The solid was dried in a vacuum. Yield: 6.28 g (10.20 mmol, 95%). Elemental analysis: calculated (%) for $C_{32}H_{83}B_{11}N_2$, C 62.50, H 13.61, N 4.56; found, C 62.31, H 13.58, N 4.21.

General protocol for the partial chlorination of $[nBu_4N]_2[closo\text{-}B_{11}H_{11}]$. $[nBu_4N]_2[closo\text{-}B_{11}H_{11}]$ was dissolved in dichloromethane and cooled to 0 °C. NCS was added to the solution and the mixture was stirred for 5 hours at 0 °C. The solution was stirred for additional 20 hours at room temperature. All volatiles were removed under reduced pressure and the remaining solid materials were dissolved in a minimum amount of acetone. The addition of water resulted in the formation of a white precipitate that was filtered off and dried in a vacuum. The ^{1}H NMR spectroscopy data of the $[n\mathrm{Bu_4N}]^+$ cation are in accordance to: ^{1}H NMR (500.1 MHz, CD_3CN): $\delta = 3.16$ (m, 8H, CH_2), 1.67 (m, 8H, CH_2), 1.41 (m, 8H, CH_2), 1.02 (t, 12H, $^{3}J(^{1}H,^{1}H) = 7.3$ Hz, CH_3). The ^{1}H and ^{11}B NMR spectroscopy data of the dianionic boron clusters are listed in Table S7 and the ^{11}B as well as $^{11}B\{^{1}H\}$ NMR spectra are shown in Figure S16. The product composition depends on the amount of NCS used, the temperature, and the reaction time. Slight variations can result in minor different product compositions.

Chlorination of $[n\mathrm{Bu_4N}]_2[\mathit{closo}\text{-}\mathrm{B_{11}H_{11}}]$ with 1.08 eq of NCS. $[n\mathrm{Bu_4N}]_2[\mathit{closo}\text{-}\mathrm{B_{11}H_{11}}]$ (160 mg, 0.26 mmol) was dissolved in dichloromethane (10 mL) and NCS (38 mg, 0.28 mmol) was added. Yield: 147 mg (contains 122 mg of $[n\mathrm{Bu_4N}]_2[\mathit{closo}\text{-}\mathrm{B_{11}ClH_{10}}]$ (72%) and 25 mg of $[n\mathrm{Bu_4N}]_2[\mathit{closo}\text{-}\mathrm{B_{11}Cl_2H_9}]$ (14%)) Elemental analysis: calculated (%) for $C_{32}H_{81.83}B_{11}Cl_{1.17}N_2$, C 58.66, H 12.59, N 4.28; found, C 58.61, H 12.52, N 4.43.

Chlorination of $[n\mathrm{Bu_4N}]_2[\mathit{closo}\text{-}\mathrm{B_{11}H_{11}}]$ with 2.12 eq of NCS. $[n\mathrm{Bu_4N}]_2[\mathit{closo}\text{-}\mathrm{B_{11}H_{11}}]$ (210 mg, 0.34 mmol) was dissolved in dichloromethane (10 mL) and NCS (95 mg, 0.72 mmol) was added. Yield: 160 mg (contains 144 mg of $[n\mathrm{Bu_4N}]_2[\mathit{closo}\text{-}\mathrm{B_{11}Cl_2H_9}]$ (66%) and 16 mg of $[n\mathrm{Bu_4N}]_2[\mathit{closo}\text{-}\mathrm{B_{11}Cl_3H_8}]$ (7%)).

Chlorination of $[n\mathrm{Bu_4N}]_2[\mathit{closo}\text{-}\mathrm{B_{11}H_{11}}]$ with 3.10 eq of NCS. $[n\mathrm{Bu_4N}]_2[\mathit{closo}\text{-}\mathrm{B_{11}H_{11}}]$ (190 mg, 0.31 mmol) was dissolved in dichloromethane (10 mL) and NCS (128 mg, 0.96 mmol) was added. Yield: 170 mg (contains 133 mg of $[n\mathrm{Bu_4N}]_2[\mathit{closo}\text{-}\mathrm{B_{11}Cl_3H_8}]$ (60%), 29 mg of $[n\mathrm{Bu_4N}]_2[\mathit{closo}\text{-}\mathrm{B_{11}Cl_2H_9}]$ (14%), and 8 mg of $[n\mathrm{Bu_4N}]_2[\mathit{closo}\text{-}\mathrm{B_{11}Cl_4H_7}]$ (3%)).

Chlorination of $[n\mathrm{Bu_4N}]_2[\mathit{closo}\text{-}\mathrm{B_{11}H_{11}}]$ with 4.10 eq of NCS. $[n\mathrm{Bu_4N}]_2[\mathit{closo}\text{-}\mathrm{B_{11}H_{11}}]$ (190 mg, 0.31 mmol) was dissolved in dichloromethane (10 mL) and NCS (170 mg, 1.27 mmol) was added. Yield: 170 mg (contains 129 mg of $[n\mathrm{Bu_4N}]_2[\mathit{closo}\text{-}\mathrm{B_{11}Cl_4H_7}]$ (55%), 24 mg of $[n\mathrm{Bu_4N}]_2[\mathit{closo}\text{-}\mathrm{B_{11}Cl_3H_8}]$ (11%), and 17 mg of $[n\mathrm{Bu_4N}]_2[\mathit{closo}\text{-}\mathrm{B_{11}Cl_5H_6}]$

(7%)). Elemental analysis: calculated (%) for $C_{32}H_{79.04}B_{11}Cl_{3.96}N_2$, C 51.16, H 10.60, N 3.73; found, C 50.80, H 10.40, N 3.86. MALDI-MS *m*/*z*: calculated for [*closo*-$B_{11}Cl_4H_7$]$^{\bullet-}$, 263(7), 264(22), 265(49), 266(81),267(100), 268 (99), 269 (83), 270(58), 271(33), 272(18); found, 263(37), 264(59), 265(84), 266(98), 267(100), 268(99), 269(92), 270(74), 271(54), 272(38).

Chlorination of [*n*Bu$_4$N]$_2$[*closo*-B$_{11}$H$_{11}$] with 5.10 eq of NCS. [*n*Bu$_4$N]$_2$[*closo*-B$_{11}$H$_{11}$] (190 mg, 0.31 mmol) was dissolved in dichloromethane (10 mL) and NCS (210 mg, 1.58 mmol) was added. Yield: 210 mg (contains 155 mg of [*n*Bu$_4$N]$_2$[*closo*-$B_{11}Cl_5H_6$] (64%), 32 mg of [*n*Bu$_4$N]$_2$[*closo*-$B_{11}Cl_6H_5$] (13%), and 23 mg of [*n*Bu$_4$N]$_2$[*closo*-$B_{11}Cl_4H_7$] (10%)). MALDI-MS *m*/*z*: calculated for [*closo*-$B_{11}Cl_5H_6$]$^{\bullet-}$, 295(>1), 296(1), 297(6), 298(18), 299(41), 300(70), 301(92), 302(100), 303(92), 304(72), 305(48), 306(29), 307(14), 308(7), 309(2), 310(1), 311(>1); found, 295(>1), 296(2), 297(6), 298(19), 299(42), 300(71), 301(93), 302(100), 303(92), 304(71), 305(47), 306(28), 307(13), 308(7), 309(2), 310(1), 311(>1).

Chlorination of [*n*Bu$_4$N]$_2$[*closo*-B$_{11}$H$_{11}$] with 6.06 eq of NCS. [*n*Bu$_4$N]$_2$[*closo*-B$_{11}$H$_{11}$] (190 mg, 0.31 mmol) was dissolved in dichloromethane (10 mL) and NCS (250 mg, 1.88 mmol) was added. Yield: 180 mg (contains 140 mg of [*n*Bu$_4$N]$_2$[*closo*-$B_{11}Cl_6H_5$] (55%), 18 mg of [*n*Bu$_4$N]$_2$[*closo*-$B_{11}Cl_7H_4$] (7%), and 22 mg of [*n*Bu$_4$N]$_2$[*closo*-$B_{11}Cl_5H_6$] (9%)). Elemental analysis: calculated (%) for $C_{32}H_{77.02}B_{11}Cl_{5.98}N_2$, C 46.82, H 9.46, N 3.41; found, C 46.47, H 9.37, N 3.64.

Chlorination of [*n*Bu$_4$N]$_2$[*closo*-B$_{11}$H$_{11}$] with 7.21 eq of NCS. [*n*Bu$_4$N]$_2$[*closo*-B$_{11}$H$_{11}$] (510 mg, 0.83 mmol) was dissolved in dichloromethane (25 mL) and NCS (800 mg, 5.99 mmol) was added. Yield: 570 mg (contains 405 mg of [*n*Bu$_4$N]$_2$[*closo*-$B_{11}Cl_7H_4$] (57%) and 165 mg [*n*Bu$_4$N]$_2$[*closo*-$B_{11}Cl_8H_3$] (22%)). Elemental analysis: calculated (%) for $C_{32}H_{75.71}B_{11}Cl_{7.29}N_2$, C 44.38, H 8.81, N 3.23; found, C 44.26, H 8.72, N 3.10. MALDI-MS *m*/*z*: calculated for [*closo*-$B_{11}Cl_7H_4$]$^{\bullet-}$ 362(<1), 363(<1), 364(1), 365(5), 366(12), 367(30), 368(54), 369(78), 370(96), 371(100), 372(91), 373(75), 374(55), 375(35), 376(21), 377(10), 378(6), 379(2), 380(1), 381(<1), 382(<1), 383(<1), 384(<1); found, 362(<1), 363(<1), 364(<1), 365(<1), 366(4), 367(16), 368(38), 369(65), 370(88), 371(100), 372(89), 373(68), 374(46), 375(47), 376(13), 377(11), 378(1), 379(<1), 380(<1), 381(<1), 382(<1), 383(<1), 384(<1).

Chlorination of [*n*Bu$_4$N]$_2$[*closo*-B$_{11}$H$_{11}$] with 8.06 eq of NCS. [*n*Bu$_4$N]$_2$[*closo*-B$_{11}$H$_{11}$] (190 mg, 0.31 mmol) was dissolved in dichloromethane (10 mL) and NCS (335 mg, 0.96 mmol) was added. Yield: 195 mg (contains 154 mg of [*n*Bu$_4$N]$_2$[*closo*-B$_{11}$Cl$_8$H$_3$] (56%), 16 mg of [*n*Bu$_4$N]$_2$[*closo*-B$_{11}$Cl$_7$H$_4$] (6%), and 25 mg [*n*Bu$_4$N]$_2$[*closo*-B$_{11}$Cl$_9$H$_2$] (9%)).

Chlorination of [*n*Bu$_4$N]$_2$[*closo*-B$_{11}$H$_{11}$] with 9.11 eq of NCS. [*n*Bu$_4$N]$_2$[*closo*-B$_{11}$H$_{11}$] (500 mg, 0.81 mmol) was dissolved in CH$_2$Cl$_2$ (25 mL) and NCS (985 mg, 7.38 mmol) was added. Yield: 580 mg (contains 499 mg of [*n*Bu$_4$N]$_2$[*closo*-B$_{11}$Cl$_9$H$_2$] (67%), 64 mg of [*n*Bu$_4$N]$_2$[*closo*-B$_{11}$Cl$_8$H$_3$] (9%), and 17 mg of [*n*Bu$_4$N]$_2$[*closo*-B$_{11}$Cl$_{10}$H] (2%)). Elemental analysis: calculated (%) for C$_{32}$H$_{74.08}$B$_{11}$Cl$_{8.92}$N$_2$, C 41.68, H 8.10, N 3.04; found, C 42.43, H 8.33, N 3.15. MALDI-MS *m*/*z*: calculated for [*closo*-B$_{11}$Cl$_9$H$_2$]$^{\bullet-}$ 430(<1), 431(<1), 432(1), 433(3), 434(8), 435(20), 436(38), 437(60), 438(82), 439(96), 440(100), 441(93), 442(79), 443(59), 444(42), 445(25), 446(16), 447(8),448(4), 449(2),450(1), 451(<1), 452(<1), 453(<1), 454(<1); found, 429(<1), 430(<1), 431(<1), 432(<1), 433(1), 434(5), 435(19),436(39), 337(62), 438(85), 439(98), 440(100), 441(97),442(77), 443(59), 444(37), 445(21), 446(10), 447(4), 448(2),449(2), 450(<1), 451(<1), 452(<1), 453(<1), 454 (<1).

Chlorination of [*n*Bu$_4$N]$_2$[*closo*-B$_{11}$H$_{11}$] with 10.46 eq of NCS. [*n*Bu$_4$N]$_2$[*closo*-B$_{11}$H$_{11}$] (950 mg, 1.55 mmol) was dissolved in dichloromethane (25 mL) and NCS (2.17 g, 16.22 mmol) was added. This reaction was stirred for 2 hours at 0°C, only, and additionally for 2.5 hours at room temperature. Yield: 1.20 g (contains 912 mg of [*n*Bu$_4$N]$_2$[*closo*-B$_{11}$Cl$_{10}$H] (61%), 228 mg of [*n*Bu$_4$N]$_2$[*closo*-B$_{11}$Cl$_9$H$_2$] (16%), and 60 mg of [*n*Bu$_4$N]$_2$[*closo*-B$_{11}$Cl$_{11}$] (4%)). Elemental analysis: calculated (%) for C$_{32}$H$_{73.14}$B$_{11}$Cl$_{9.86}$N$_2$, C 40.27, H 7.72, N 2.94; found, C 40.77, H 7.69, N 3.08.

Preparation of [*n*Bu$_4$N]$_2$[*closo*-B$_{11}$Cl$_{11}$] with *tert*-butyl hypochlorite. [*n*Bu$_4$N]$_2$[*closo*-B$_{11}$Cl$_{10}$H] (300 mg, 0.32 mmol) was dissolved in acetonitrile (14 mL) and cooled to 0°C. *tert*-Butyl hypochlorite (0.08 mL, 77 mg, 068 mmol) was added in the dark and the solution was stirred at 0 °C for 8.5 hours. Then the solution was stirred for two days at room temperature. The solvent was removed under reduced pressure and the remaining solid was dissolved in acetone (2 mL). A yellowish precipitate formed upon addition of water (2 mL) that was filtered off and dried in a vacuum. Yield: 260 mg (contains 174 mg of $[n\text{Bu}_4\text{N}]_2[closo\text{-B}_{11}\text{Cl}_{11}]$ (55%) and 86 mg of $[n\text{Bu}_4\text{N}]_2[closo\text{-B}_{10}\text{Cl}_{10}]$ (28%)). Elemental analysis: calculated (%) for $C_{32}H_{72}B_{10.67}Cl_{10.67}N_2$, C 39.28, H 7.42, N 2.86; found, C 38.67, H 7.44, N 3.00. MALDI-MS *m*/*z*: calculated for $[closo\text{-B}_{11}\text{Cl}_{11}]^{\bullet-}$ 498 (<1), 499 (<1), 500(<1), 501(2), 502(5), 503(13), 504(27), 505(45), 506(66), 507(85), 508(97), 509(100), 510(94), 511(80), 512(64), 513(46), 514(31), 515(19), 516(12), 517(6), 518(3), 519(1), 520(1), 521 (<1), 522 (<1), 523 (<1), 524 (<1); found, 498(<1), 499(<1), 500(<1), 501(<1), 502(<1), 503(2), 504(9), 505(26), 506(57), 507(77), 508(99), 509(100), 510(96), 511(67), 512(45), 513(27), 514(13), 515(3), 516(<1), 517(<1), 518(<1), 519(<1), 520(<1), 521(<1), 522(<1), 523(<1), 524(<1); main peak for $[closo\text{-B}_{10}\text{Cl}_{10}]^{\bullet-}$: 462 (85).

Preparation of $[n\text{Bu}_4\text{N}]_2[closo\text{-B}_{11}\text{Cl}_{11}]$ with NCS. $[n\text{Bu}_4\text{N}]_2[closo\text{-B}_{11}\text{H}_{11}]$ (2.00 g, 3.25 mmol) were dissolved in dichloromethane (60 mL) and cooled to 0 °C. NCS (8.62 g, 64.54 mmol) was added and the mixture was stirred for 2 hours at 0 °C followed by stirring at room temperature for 2 more hours. The solvent was removed under reduced pressure and the solid remainder was dissolved in acetone (50–100 mL). The addition of water (500 mL) resulted in the formation of an orange precipitate, which was filtered off. The solid was washed with diethyl ether (100 mL) and dried in a vacuum. Yield: 2.65 g (contains 1.62 g of $[n\text{Bu}_4\text{N}]_2[closo\text{-B}_{11}\text{Cl}_{11}]$ (50%), 716 mg of $[n\text{Bu}_4\text{N}]_2[closo\text{-B}_{10}\text{Cl}_{10}]$ (23%), and 318 mg of $[n\text{Bu}_4\text{N}]_2[closo\text{-B}_{11}\text{Cl}_{10}\text{H}]$ (10%)).

General protocol for the synthesis of $[n\text{Bu}_4\text{N}]^+$ salts of mixed brominated/ chlorinated *closo*-undecarborate anions. The $[n\text{Bu}_4\text{N}]^+$ salts of the partially chlorinated *closo*-undecarborate anions were dissolved in dichloromethane and the solutions were cooled to 0 °C. A solution of bromine and dichloromethane was added to the this solution. The mixture was stirred at 0°C for 5 hours and additionally for 18 hours at room temperature. All volatiles were removed under reduced pressure and the solid residue was dissolved in acetone. An aqueous solution of sodium sulfite solution was added, which resulted in the precipitation of a solid that was filtered off and dried in a vacuum. Selected ^{11}B NMR spectra of the mixed halogenated anions are depicted in Figure S15.

Bromination of [*n*Bu$_4$N]$_2$[*closo*-B$_{11}$Cl$_6$H$_5$] and [*n*Bu$_4$N]$_2$[*closo*-B$_{11}$Cl$_7$H$_4$]. A mixture of [*n*Bu$_4$N]$_2$[*closo*-B$_{11}$Cl$_6$H$_5$] (80%) and [*n*Bu$_4$N]$_2$[*closo*-B$_{11}$Cl$_7$H$_4$] (20%) (200 mg, 0.19 mmol) was dissolved in dichloromethane (12 mL) and a freshly prepared solution of bromine in dichloromethane (1.95 M, 0.80 mL) was added. Yield: 200 mg (contains 160 mg of [*n*Bu$_4$N]$_2$[*closo*-B$_{11}$Cl$_6$Br$_5$] (69%) and 40 mg of [*n*Bu$_4$N]$_2$[*closo*-B$_{11}$Cl$_7$Br$_4$] (18%)). Elemental analysis: calculated (%) for $C_{32}H_{72}B_{11}Br_{4.8}Cl_{6.2}N_2$, C 31.84, H 6.01, N 2.32; found, C 30.71, H 5.84, N 3.02.

Bromination of [*n*Bu$_4$N]$_2$[*closo*-B$_{11}$Cl$_7$H$_4$] and [*n*Bu$_4$N]$_2$[*closo*-B$_{11}$Cl$_8$H$_3$]. A mixture of [*n*Bu$_4$N]$_2$[*closo*-B$_{11}$Cl$_7$H$_4$] (71%) and [*n*Bu$_4$N]$_2$[*closo*-B$_{11}$Cl$_8$H$_3$] (29%) (200 mg, 0.17 mmol) was dissolved in dichloromethane (12 mL) and a freshly prepared solution of bromine in dichloromethane (1.95 M, 0.60 mL) was added. Yield: 200 mg (contains 142 mg of [*n*Bu$_4$N]$_2$[*closo*-B$_{11}$Cl$_7$Br$_4$] (71%) and 58 mg of [*n*Bu$_4$N]$_2$[*closo*-B$_{11}$Cl$_8$Br$_3$] (30%)). Elemental analysis: calculated (%) for $C_{32}H_{72}B_{11}Br_{3.71}Cl_{7.29}N_2$, C 33.17, H 6.26, N 2.42; found, C 32.69, H 6.21, N 2.50 MALDI-MS *m*/*z*: calculated for [*closo*-B$_{11}$Br$_4$Cl$_7$]$^{\bullet-}$ 676(<1), 677(<1), 678(1), 679(4), 680(9), 681(18), 682(31), 683(48), 684(67), 685(84), 686(96), 687(100), 688(96), 689(84), 690(69), 691(50), 692(36), 693(22), 694(13), 695(7), 696(4), 697(1), 698(1), 699(<1), 700(<1); found, 676 (<1), 677(<1), 678 (<1), 679 (<1), 680(1), 681(8), 682(21), 683(38), 684(60), 685(81), 686(93), 687(100), 688(90), 689(79), 690(62), 691(39), 692(22), 693(11), 694(4), 695(1), 696(<1), 697(<1), 698(<1), 699 (<1), 700 (<1).; main peak for [*closo*-B$_{11}$Br$_3$Cl$_8$]$^{\bullet-}$: 642(53).

Bromination of [*n*Bu$_4$N]$_2$[*closo*-B$_{11}$Cl$_8$H$_3$] and [*n*Bu$_4$N]$_2$[*closo*-B$_{11}$Cl$_9$H$_2$]. A mixture of [*n*Bu$_4$N]$_2$[*closo*-B$_{11}$Cl$_8$H$_3$] (85%) and [*n*Bu$_4$N]$_2$[*closo*-B$_{11}$Cl$_9$H$_2$] (15%) (200 mg, 0.20 mmol) was dissolved in dichloromethane (12 mL) and a freshly prepared solution of bromine in dichloromethane (1.95 M, 0.59 mL) was added. Yield: 165 mg (contains 140 mg of [*n*Bu$_4$N]$_2$[*closo*-B$_{11}$Cl$_8$Br$_3$] (62%) and 25 mg of [*n*Bu$_4$N]$_2$[*closo*-B$_{11}$Cl$_9$Br$_2$] (12%)). Elemental analysis: calculated (%) for $C_{32}H_{72}B_{11}Br_{2.85}Cl_{8.15}N_2$, C 34.30, H 6.48, N 2.50; found, C 33.82, H 6.42, N 2.53 MALDI-MS *m*/*z*: calculated for [*closo*-B$_{11}$Br$_3$Cl$_8$]$^{\bullet-}$ 631 (<1), 632 (<1), 633 (<1), 634 (1), 635 (2),636(5), 637(12), 638(22), 639(38), 640(57), 641(76), 642(92), 643(100), 644(99), 645(91), 646(76), 647(59), 648(41), 649(28), 650(16), 651(10), 652(5), 653(2), 654(1), 655(<1), 656(<1), 657(<1), 658(<1); found, 631(<1), 632(<1), 633(<1), 634(<1), 635(1), 636(3), 637(13), 638(26), 639(46), 640(69), 641(85), 642(94), 643(100), 644(92), 645(72), 646(52), 647(32), 648(18), 649(8), 650(2), 651(<1), 652(<1), 653(<1), 654(<1), 655(<1), 656(<1); main peak for [*closo*-$B_{11}Br_2Cl_9$]$^{•-}$: 598(12).

Bromination of [*n*Bu_4N]$_2$[*closo*-$B_{11}Cl_9H_2$], [*n*Bu_4N]$_2$[*closo*-$B_{11}Cl_8H_3$], and [*n*Bu_4N]$_2$[*closo*-$B_{11}Cl_{10}H$]. A mixture of [*n*Bu_4N]$_2$[*closo*-$B_{11}Cl_9H_2$] (86%), [*n*Bu_4N]$_2$[*closo*-$B_{11}Cl_8H_3$] (11%), and [*n*Bu_4N]$_2$[*closo*-$B_{11}Cl_{10}H$] (3%) (200 mg, 0.19 mmol) was dissolved in dichloromethane (12 mL) and a freshly prepared solution of bromine in dichloromethane (1.95 M, 0.36 mL) was added. Yield: 190 mg (contains 163 mg of [*n*Bu_4N]$_2$[*closo*-$B_{11}Cl_9Br_2$] (79%), 21 mg of [*n*Bu_4N]$_2$[*closo*-$B_{11}Cl_8Br_3$] (10%), and 6 mg of [*n*Bu_4N]$_2$[*closo*-$B_{11}Cl_{10}Br$] (3%)). Elemental analysis: calculated (%) for $C_{32}H_{72}B_{11}Br_{2.08}Cl_{8.92}N_2$, C 35.38, H 6.68, N 2.58; found, C 35.40, H 6.76, N 2.65 MALDI-MS *m*/*z*: calculated for [*closo*-$B_{11}Br_2Cl_9$]$^{•-}$ 587(<1), 588(<1), 589(1), 590(3), 591(7), 592(15), 593(29), 594(47), 595(66), 596(84), 597(96), 598(100), 599(95), 600(82), 601(66), 602(49), 603(32), 604(21), 605(12), 606(7), 607(3), 608(2), 609(1), 610(<1), 611(<1), 612(<1); found, 587(<1), 588(<1), 589(<1), 590(<1), 591(1), 592(4), 593(14), 594(30), 595(54), 596(76), 597(97), 598(100), 599(93), 600(82), 601(55), 602(33), 603(18), 604(8), 605(2), 606(1), 607(<1), 608(<1), 609(<1), 610(<1), 611(<1), 612(<1); main peak for [*closo*-$B_{11}Br_3Cl_8$]$^{•-}$: 642(7).

Bromination of a mixture of [*n*Bu_4N]$_2$[*closo*-$B_{11}Cl_{10}H$], [*n*Bu_4N]$_2$[*closo*-$B_{11}Cl_{11}$], and [*n*Bu_4N]$_2$[*closo*-$B_{10}Cl_{10}$]. A mixture of [*n*Bu_4N]$_2$[*closo*-$B_{11}Cl_{10}H$] (83%), [*n*Bu_4N]$_2$[*closo*-$B_{11}Cl_{11}$] (12%), and [*n*Bu_4N]$_2$[*closo*-$B_{10}Cl_{10}$] (5%) (510 mg, 0.44 mmol) was dissolved in dichloromethane (25 mL) and a freshly prepared solution of bromine in dichloromethane (1.17 M, 0.9 mL) was added. Yield: 475 mg (contains 394 mg of [*n*Bu_4N]$_2$[*closo*-$B_{11}Cl_{10}Br$] (86%), 57 mg of [*n*Bu_4N]$_2$[*closo*-$B_{11}Cl_{11}$] (13%), and 24 mg of [*n*Bu_4N]$_2$[*closo*-$B_{10}Cl_{10}$] (6%)). Elemental analysis: calculated (%) for $C_{32}H_{72}B_{10.95}Br_{0.83}Cl_{10.12}N_2$, C 37.37, H 7.06, N 2.72; found, C 38.17, H 7.17, N 2.94 MALDI-MS *m*/*z*: calculated for [*closo*-$B_{11}BrCl_{10}$]$^{•-}$ 543(<1), 544(<1), 545(1), 546(4), 547(10), 548(21), 549(37), 550(56), 551(76), 552(92), 553(100), 554(97), 555(89), 556(74), 557(56), 558(40), 559(25), 560(16), 561(8), 562(5), 563(2), 564(1), 565(<1), 566(<1), 567(<1); found, 543(<1), 544(<1), 545(<1), 546(<1), 547(1), 548(8), 549(21), 550(42), 551(71), 552(89), 553(100), 554(97), 555(76), 556(57), 557(36), 558(21), 559(9), 560(3), 561(1), 562(<1), 563(<1), 564(<1), 565(<1), 566(<1), 567(<1); main peak for [*closo*-$B_{11}Cl_{11}$]$^{\bullet-}$: 509(15).

General protocol for the synthesis of [*n*Bu_4N]$^+$ salts of mixed iodinated/chlorinated *closo*-undecarborate anions using elemental iodine. The [*n*Bu_4N]$^+$ salts of the partially chlorinated *closo*-undecarborate anions were dissolved in dichloromethane and elemental iodine was added. The resulting solution was stirred for 3 days at 70 °C. The solvent was removed under reduced pressure and the solid remainder was dissolved in acetone. During the addition of an aqueous solution of sodium sulfite a precipitate formed, which was filtered off and dried in a vacuum. Selected ^{11}B NMR spectra of the mixed halogenated anions are depicted in Figure S15.

Iodination of [*n*Bu_4N]$_2$[*closo*-$B_{11}Cl_6H_5$] and [*n*Bu_4N]$_2$[*closo*-$B_{11}Cl_7H_4$]. A mixture of [*n*Bu_4N]$_2$[*closo*-$B_{11}Cl_6H_5$] (80%) and [*n*Bu_4N]$_2$[*closo*-$B_{11}Cl_7H_4$] (20%) (150 mg, 0.14 mmol) was dissolved in dichloromethane (12 mL) and iodine (460 mg, 1.81 mmol) was added. Yield: 190 mg (contains 152 mg of [*n*Bu_4N]$_2$[*closo*-$B_{11}Cl_6I_5$] (75%) and 38 mg of [*n*Bu_4N]$_2$[*closo*-$B_{11}Cl_7Br_4$] (20%)). Elemental analysis: calculated (%) for $C_{32}H_{72}B_{11}Cl_{6.20}I_{4.8}N_2$, C 26.83, H 5.07, N 1.96; found, C 25.08, H 4.76, N 1.98 MALDI-MS *m*/*z*: calculated for [*closo*-$B_{11}Cl_6I_5$]$^{\bullet-}$ 959(<1), 960(1), 961(5), 962(15), 963(35), 964(62), 965(86), 966(100), 967(99), 968(85), 969(63), 970(43), 971(24), 972(13), 973(5), 974(3), 975(1), 976(<1); found, 959(<1), 960(1), 961(7), 962(29), 963(61), 964(87), 965(98), 966(100), 967(88), 968(62), 969(40), 970(17), 971(7), 972(1), 973(<1), 974(<1), 975(<1); main peak for [*closo*-$B_{11}Cl_7I_4$]$^{\bullet-}$: 876(37).

Iodination of [*n*Bu_4N]$_2$[*closo*-$B_{11}Cl_7H_4$] and [*n*Bu_4N]$_2$[*closo*-$B_{11}Cl_8H_3$]. A mixture of [*n*Bu_4N]$_2$[*closo*-$B_{11}Cl_7H_4$] (71%) and [*n*Bu_4N]$_2$[*closo*-$B_{11}Cl_8H_3$] (29%) (150 mg, 0.13 mmol) was dissolved in dichloromethane (12 mL) and iodine (370 mg, 1.46 mmol) was added. Yield: 120 mg (contains 85 mg of [*n*Bu_4N]$_2$[*closo*-$B_{11}Cl_7I_4$] (48%) and 35 mg of [*n*Bu_4N]$_2$[*closo*-$B_{11}Cl_8I_3$] (21%)). Elemental analysis: calculated (%) for $C_{32}H_{72}B_{11}Cl_{7.29}I_{3.71}N_2$, C 28.83, H 5.44, N 2.10; found, C 28.00, H 5.35, N 2.21 MALDI-MS *m*/*z*: calculated for [*closo*-$B_{11}Cl_7I_4$]$^{\bullet-}$ 868(<1), 869(1), 870(4), 871(12), 872(29), 873(52), 874(77), 875(94), 876(100), 877(92), 878(75), 879(55), 880(34), 881(21), 882(13), 883(4), 884(1), 885(<1), 886(<1), 887(<1); found, 868(<1), 869(<1), 870(1), 871(8), 872(44), 873(68), 874(96), 875(100), 876(88), 877(68), 878(48), 879(24), 880(12), 881(4), 882(1), 883(<1), 884(<1), 885(<1), 886(<1); main peak for [*closo*-$B_{11}Cl_8I_3$]$^{\bullet-}$: 783(45).

Iodination of [*n*Bu_4N]$_2$[*closo*-$B_{11}Cl_8H_3$] and [*n*Bu_4N]$_2$[*closo*-$B_{11}Cl_9H_2$]. A mixture of [*n*Bu_4N]$_2$[*closo*-$B_{11}Cl_8H_3$] (85%) and [*n*Bu_4N]$_2$[*closo*-$B_{11}Cl_9H_2$] (15%) (150 mg, 0.15 mmol) was dissolved in dichloromethane (8 mL) and iodine (300 mg, 1.18 mmol) was added. Yield: 170 mg (contains 145 mg of [*n*Bu_4N]$_2$[*closo*-$B_{11}Cl_8I_3$] (76%) and 25 mg of [*n*Bu_4N]$_2$[*closo*-$B_{11}Cl_9I_2$] (14%)). Elemental analysis: calculated (%) for $C_{32}H_{72}B_{11}Cl_{8.15}I_{2.85}N_2$, C 30.64, H 5.79, N 2.23; found, C 30.40, H 5.71, N 2.31 MALDI-MS *m*/*z*: calculated for [*closo*-$B_{11}Cl_8I_3$]$^{\bullet-}$ 774(<1), 775(<1), 776(1), 777(3), 778(10), 779(24), 780(45), 781(69), 782(89), 783(100), 784(9), 785(86), 786(68), 787(47), 788(31), 789(17), 790(10), 791(4), 792(2), 793(<1), 794(<1), 795(<1), 796(<1); found, 775(<1), 776(<1), 777(1), 778(7), 779(23), 780(46), 781(72), 782(91), 783(100), 784(99), 785(88), 786(70), 787(47), 788(30), 789(13), 790(6), 791(1), 792(<1), 793(<1), 794(<1), 795(<1), 796(<1); main peak for [*closo*-$B_{11}Cl_9I_2$]$^{\bullet-}$: 692(20).

Iodination of [*n*Bu_4N]$_2$[*closo*-$B_{11}Cl_9H_2$], [*n*Bu_4N]$_2$[*closo*-$B_{11}Cl_8H_3$], and [*n*Bu_4N]$_2$[*closo*-$B_{11}Cl_{10}H$]. A mixture of [*n*Bu_4N]$_2$[*closo*-$B_{11}Cl_9H_2$] (86%), [*n*Bu_4N]$_2$[*closo*-$B_{11}Cl_8H_3$] (11%), and [*n*Bu_4N]$_2$[*closo*-$B_{11}Cl_{10}H$] (3%) (150 mg, 0.14 mmol) was dissolved in dichloromethane (8 mL) and iodine (370 mg, 1.46 mmol) was added. Yield: 120 mg (contains 103 mg of [*n*Bu_4N]$_2$[*closo*-$B_{11}Cl_9I_2$] (63%), 13 mg of [*n*Bu_4N]$_2$[*closo*-$B_{11}Cl_8I_3$] (7%), and 4 mg of [*n*Bu_4N]$_2$[*closo*-$B_{11}Cl_{10}I$] (3%)). Elemental analysis: calculated (%) for $C_{32}H_{72}B_{11}Cl_{8.92}I_{2.08}N_2$, C 32.46, H 6.13, N 2.37; found, C 32.48, H 6.11, N 2.47. MALDI-MS *m*/*z*: calculated for [*closo*-$B_{11}I_2Cl_9$]$^{\bullet-}$ 682(<1), 683(<1), 684(1), 685(3), 686(8), 687(20), 688(38), 689(60), 690(82), 691(96), 692(100), 693(93), 694(79), 695(59), 696(42), 697(26), 698(16), 699(8), 700(4), 701(2), 702(1), 703(<1), 704(<1), 705(<1), 706 (<1); found, 682(<1), 683(<1), 684(<1), 685(1), 686(4), 687 (13), 688(31), 689(56), 690(82), 691(99), 692(100), 693(94), 694(74), 695(51), 696(36), 697(18), 698(9), 699(3), 700(2), 701(<1), 702(<1), 703(<1), 704(<1), 705(<1), 706(<1); main peak for [*closo*-$B_{11}I_3Cl_8$]$^{\bullet-}$: 715(9).

Iodination of a mixture of [*n*Bu$_4$N]$_2$[*closo*-B$_{11}$Cl$_{10}$H] and [*n*Bu$_4$N]$_2$[*closo*-B$_{11}$Cl$_{11}$]. A mixture of [*n*Bu$_4$N]$_2$[*closo*-B$_{11}$Cl$_{10}$H] (79%) and [*n*Bu$_4$N]$_2$[*closo*-B$_{11}$Cl$_{11}$] (21%) was dissolved in dichloromethane (15 mL) and a solution of iodine monochloride in dichloromethane (0.49 M, 1.65 mL) was added. The resulting solution was stirred at room temperature for 18 hours. The solvent was removed under reduced pressure and the solid obtained was dissolved in acetone. The addition of water (200 mL) yielded a precipitate that was filtered off and washed with an aqueous solution of sodium sulfite and water. The solid was dried in a vacuum. Yield: 430 mg (contains 340 mg of [*n*Bu$_4$N]$_2$[*closo*-B$_{11}$Cl$_{10}$I] (76%) and 90 mg of [*n*Bu$_4$N]$_2$[*closo*-B$_{11}$Cl$_{11}$] (22%)). Elemental analysis: calculated (%) for $C_{32}H_{72}B_{11}Cl_{10.21}I_{2.79}N_2$, C 36.05, H 6.81, N 2.63; found, C 36.48, H 6.81, N 2.81 MALDI-MS *m*/*z*: calculated for [*closo*-B$_{11}$ICl$_{10}$]$^{\bullet-}$ 590(<1), 591(<1), 592(<1), 593(2), 594(7), 595(16), 596(32), 597(53), 598(74), 599(92), 600(100), 601(99), 602(88), 603(71), 604(53), 605(35), 606(23), 607(13), 608(7), 609(3), 610(2), 611(1), 612(<1), 613(<1), 614(<1), 615 (<1); found, 589(<1), 590(<1), 591(<1), 592(<1), 593(2), 594(7), 595 (18), 596(33), 597(54), 598(77), 599(92), 600(100), 601(98), 602(87), 603(70), 604(52), 605(34), 606(22), 607(12), 608(8), 609(3), 610(2), 611(1), 612(<1), 613(<1), 614 (<1), 615(<1); main peak for [*closo*-B$_{11}$Cl$_{11}$]$^{\bullet-}$: 509(12).

Preparation of [*n*Bu$_4$N]$_2$[*closo*-B$_{10}$Cl$_{10}$]. The preparation is described in the method section of the main text. Elemental analysis: calculated (%) for $C_{32}H_{72}B_{10}Cl_{10}N_2$, C 40.56, H 7.66, N 2.96; found, C 40.68, H 7.51, N 3.02. {^{11}B} NMR (160.46 MHz, CD$_3$CN): δ = –3.3 (s, 2B, B1+12), –10.5 (s, 10B, B2-11) ppm MALDI-MS *m*/*z*: calculated for [*closo*-B$_{10}$Cl10]$^{\bullet-}$ 453(<1), 454(<1), 455(1), 456(5), 457(13), 458(28), 459(48), 460(70), 461(89), 462 (100), 463 (100), 464(91), 465(74), 466(57), 467(38), 468(25), 469(14), 470 (8), 471(4), 472(2), 473(1), 474(<1), 475(<1),476(<1), 477(<1); found, 453(<1), 454(<1), 455(1), 456(1), 457(10), 458(27), 459(51), 460(79), 461(93), 462(100), 463(99), 464(90), 465(74), 466(54), 467(32), 468(19), 469(8), 470(4), 471(1), 472(<1), 473(<1), 474(<1), 475(<1), 476(<1), 477(<1), 478(<1); main peak for [*closo*-B$_{11}$Cl$_{11}$]$^{\bullet-}$: 509(3).

Preparation of [Et$_3$NH]$_2$[*closo*-B$_{10}$Br$_{10}$]. [Et$_3$NH]$_2$[*closo*-B$_{10}$H$_{10}$] (1.00 g, 3.09 mmol) was dissolved in water/ethanol (60 mL, 50:50 v/v). Subsequently, bromine (3 mL, 9.30 g, 58.20 mmol) was added. The solution was stirred over night at 100 °C and 24 hours at room temperature. Most of the ethanol was removed at reduced pressure and the resulting precipitate was isolated by filtration and dried in a vacuum. Yield: 2.68 g (2.41 mmol, 78%). ^{11}B NMR (128.46 MHz, CD_3CN): δ = –2.3 (s, 2B, B1+10), −12.9 (s, 10B, B2–9) ppm.

Preparation of [*n*Bu$_4$N]$_2$[*closo*-B$_{10}$Br$_{10}$]. [Et_3NH]$_2$[*closo*-$B_{10}Br_{10}$] (500 mg, 0.44 mmol) was dissolved in an aqueous KOH solution (100 mL, 10%). A solution of [*n*Bu_4N]Br (312 mg, 0.97 mmol) in a minimum of water was added to the solution, which resulted in the precipitation of [*n*Bu_4N]$_2$[*closo*-$B_{10}Br_{10}$] that was isolated by filtration and dried in a vacuum. Yield: 0.53 g (0.38 mmol, 86%). Elemental analysis: calculated (%) for $C_{32}H_{72}B_{10}Br_{10}N_2$, C 27.61, H 5.21, N 2.01; found, C 27.42, H 5.02, N 2.21. ^{11}B NMR (128.46 MHz, CD_3CN): δ = –2.2 (s, 2B, B1+10), –12.9 (s, 10B, B2–9) ppm.

Preparation of [*n*Bu$_4$N]$_2$[*closo*-B$_{10}$I$_{10}$]. [Et_3NH]$_2$[*closo*-$B_{10}H_{10}$] (500 g, 1.55 mmol) was dissolved in methanol. Iodine (2.50 g, 9.85 mmol) and iodine monochloride (5.03 g, 30.98 mmol) were added. The solution was stirred at 80 °C for 6 days. The solvent was removed under vacuum. The solid remainder was dissolved in an aqueous KOH solution (100 mL, 10%) and the solution was filtered. A solution of [*n*Bu_4N]Br (1.10 mg, 3.46 mmol) in a minimum of water was added to the clear solution upon which solid [*n*Bu_4N]$_2$[*closo*-$B_{10}I_{10}$] formed. The solid was isolated by filtration and dried in a vacuum. Yield: 1.69 g (0.91 mmol, 59%). Elemental analysis: calculated (%) for $C_{32}H_{72}B_{10}I_{10}N_2$, C 20.64, H 3.90, N 1.50; found, C 21.49, H 3.95, N 1.48. ^{11}B NMR (128.46 MHz, CD_3CN): δ = –2.9 (s, 2B, B1+10), –20.2 (s, 10B, B2–9) ppm.

Preparation of [*n*Bu$_4$N]$_2$[*closo*-B$_{11}$Br$_{11}$]. [*n*Bu_4N]$_2$[*closo*-$B_{11}H_{11}$] (2.00 g, 3.25 mmol) was dissolved in dichloromethane (20 mL) and the solution was cooled to 0 °C. A solution of bromine (12.4 g, 77.6 mmol) in dichloromethane was added and the reaction mixture was stirred for 2 hours at 0 °C. The solution was stirred for an additional 24 hours at room temperature. An aqueous solution of sodium sulfite was added until the mixture became colourless. The dichloromethane was removed under reduced pressure und the suspension was filtered. The solid material was washed with water (100 mL) and dried in a vacuum. Yield: 3.80 g (2.56 mmol, 79%). Elemental analysis: calculated (%) for

$C_{32}H_{72}B_{11}Br_{11}N_2$, C 25.92, H 4.89, N 1.89; found, C 26.20, H 5.07, N 1.94. ^{11}B NMR (160.46 MHz, CD_3CN): δ = –7.5 (s, 11B, B1–11) ppm.

Preparation of [*n*Bu$_4$N]$_2$[*closo*-$B_{11}I_{11}$]. [*n*Bu$_4$N]$_2$[*closo*-$B_{11}H_{11}$] (106 mg, 0.17 mmol) was dissolved in CH_2Cl_2 (6 mL). Subsequently, a solution of iodine (835 mg, 3.31mmol) in dichloromethane (4 mL) was added. The clear reaction mixture was heated to 60 °C for 55 hours. After cooling to room temperature, the solvent was removed under reduced pressure. The solid residue was dissolved in acetone (2 mL). Addition of an aqueous solution of sodium sulfite solution resulted in a precipitate that was filtered off and dried in vacuum. Yield: 200 mg (0.10 mmol, 59%). Elemental analysis: calculated (%) for $C_{32}H_{72}B_{11}I_{11}N_2$, C 19.22, H 3.63, N 1.40; found, C 19.96, H 3.69, N 1.61. ^{11}B NMR (160.46 MHz, CD_3CN): δ = –13.4 (s, 11B, B1–11) ppm MALDI-MS *m*/*z*: calculated for [*closo*-$B_{10}I_{11}$]$^{\bullet-}$ 1508(<1), 1509(<1), 1510(1), 1511(3), 1512(13), 1513(37),1514(74), 1515(100), 1516(81), 1517(30); found, 1508(<1), 1509(<1), 1510(<1), 1511(<1), 1512(5), 1513 (25), 1514(66), 1515(100), 1516(81), 1517(24).

Preparation of [*n*Bu$_4$N]$_2$[*closo*-$B_{12}Cl_{12}$]. Cs_2[*closo*-$B_{12}H_{12}$] (400 mg, 0.98 mmol) was dissolved in water (50 mL) and chlorine gas was bubbled through the solution for 5 hours at 100 °C. The solution was stirred over night at 100 °C and excess of chlorine gas was removed in vacuum at room temperature. A solution of [*n*Bu$_4$N]Br (695 mg, 2.16 mmol) in a minimum of water was added to the solution. Solid [*n*Bu$_4$N]$_2$[*closo*-$B_{12}Cl_{12}$] was isolated by filtration and dried in vacuum. Yield: 512 mg (0.49 mmol, 50%). ^{11}B NMR (128.46 MHz, CD_3CN): δ = –12.7 (s, 12B, B1–12) ppm. Elemental analysis: calculated (%) for $C_{32}H_{72}B_{11}Cl_{11}N_2$, C 36.95, H 6.97, N 2.69; found, C 37.28, H 7.22, N 2.88.

Preparation of [*n*Bu$_4$N]$_2$[*closo*-$B_{12}Br_{12}$]. Cs_2[*closo*-$B_{12}H_{12}$] (400 mg, 0.98 mmol) was dissolved in water/methanol (25 mL, 50:50 v/v). Bromine (1 mL, 3.10 g, 19.40 mmol) was added at 0 °C. The mixture was stirred for 1 hour and was allowed to warm up to room temperature. A second fraction of bromine (1.5 mL, 4.65 g, 29.10 mmol) was added at room temperature and the solution was heated to 80 °C over night. The mixture was cooled to room temperature and sodium sulfite was added until the solution became colourless. A solution of [*n*Bu$_4$N]Br (695 mg, 2.16 mmol) was added to the solution. [*n*Bu$_4$N]$_2$[*closo*-$B_{12}Br_{12}$] was isolated by filtration and dried in vacuum. Yield: 1.43 g (0.91

mmol, 92%). ^{11}B NMR (128.46 MHz, CD_3CN): $\delta = -12.7$ (s, 12B, B1–12) ppm. Elemental analysis: calculated (%) for $C_{32}H_{72}B_{11}Br_{11}N_2$, C 25.92, H 4.89, N 1.89; found, C 26.20, H 5.07, N 1.93.

Preparation of $[n\mathrm{Bu_4N}]_2[closo\text{-}\mathrm{B_{12}I_{12}}]$. Cs_2[*closo*-$B_{12}H_{12}$] (400 mg, 0.98 mmol) was dissolved in tetrachloroethane (50 mL). Iodine (1.50 g, 5.82 mmol) and iodine monochloride (2.83 g, 17.46 mmol) were added. The suspension was stirred at 180 °C for three days, cooled to room temperature and filtered. The solid material was washed with dichloromethane (2 × 50 mL). Then it was dissolved in an aqueous solution of KOH (100 mL, 10%). A solution of [*n*Bu_4N]Br (695 mg, 2.16 mmol) in a minimum of water was added, resulting in the precipitation of [*n*Bu_4N]$_2$[*closo*-$B_{12}I_{12}$]. The borate was isolated by filtration and dried in a vacuum. Yield: 1.10 g (0.52 mmol, 53%). ^{11}B NMR (128.46 MHz, CD_3CN): $\delta = -16.0$ (s, 12B, B1–12) ppm. Elemental analysis: calculated (%) for $C_{32}H_{72}B_{12}I_{12}N_2$, C 17.98, H 3.40, N 1.31; found, C 18.35, H 3.40, N 1.33.

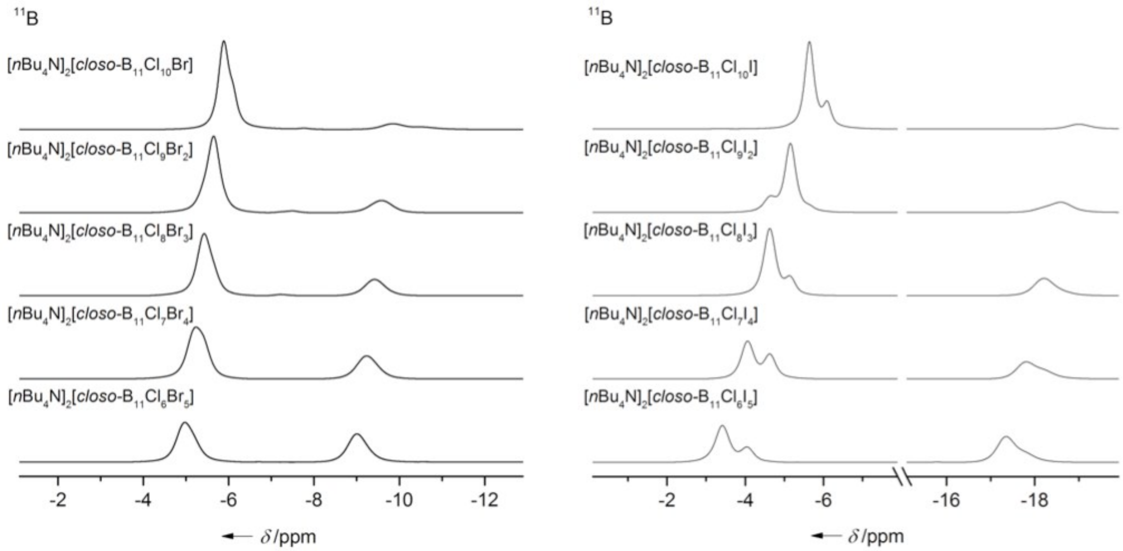

Figure S15. ^{11}B NMR spectra of the mixtures of the [*n*Bu_4N]$^+$ salts of the perhalogenated {*closo*-B_{11}} clusters [*closo*-$B_{11}Cl_xBr_{11-x}$]$^{2-}$ (x = 6–10) and [*closo*-$B_{11}Cl_xI_{11-x}$]$^{2-}$ (x = 6–10) in CD_3CN.

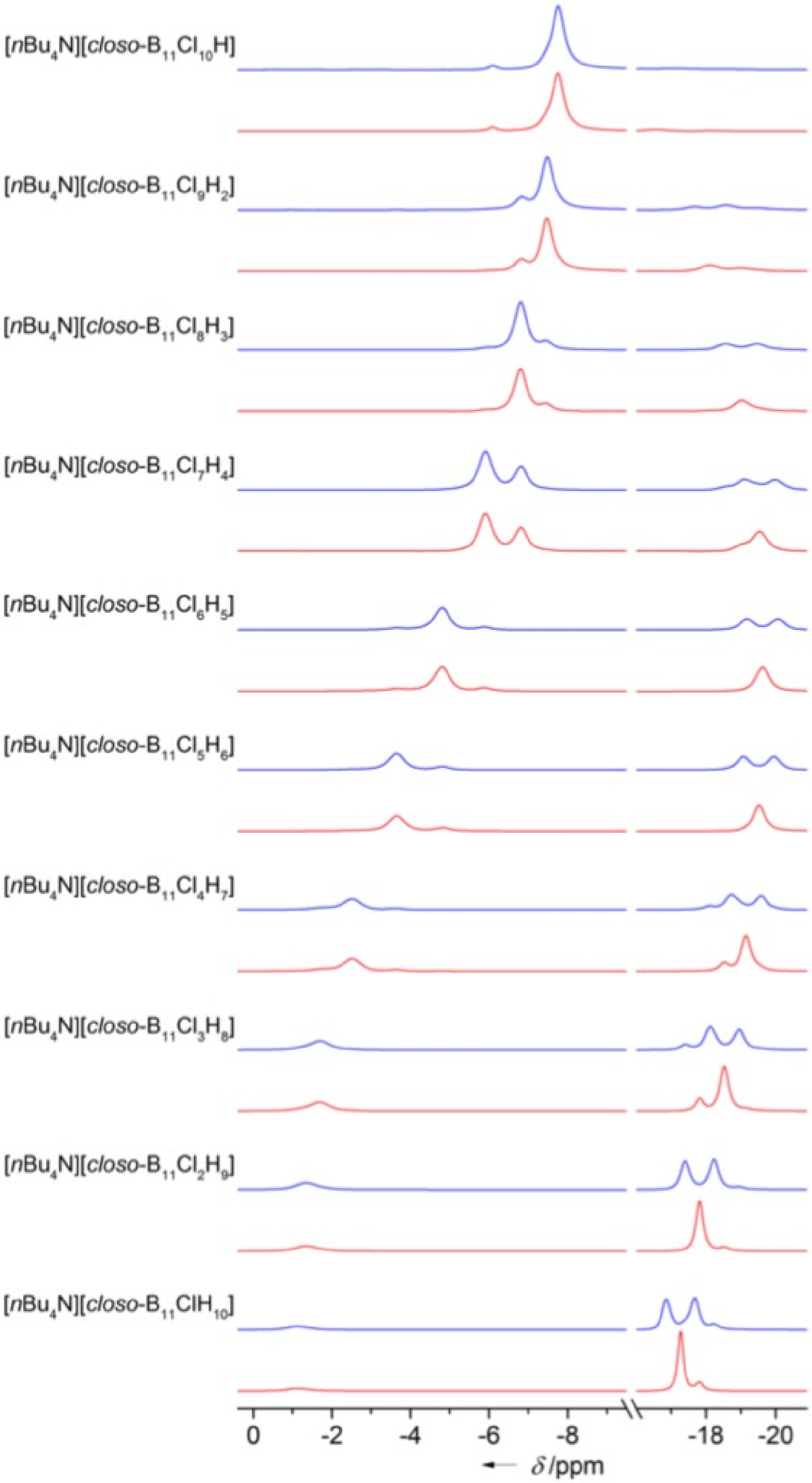

Figure S16. ^{11}B (blue) and $^{11}B\{^{1}H\}$ NMR spectra (red) of the mixtures of the $[nBu_4N]^+$ salts of partially chlorinated {*closo*-B_{11}} clusters [*closo*-$B_{11}Cl_xH_{11-x}]^{2-}$ (x = 1–10) in CD_3CN derived from $[nBu_4N]_2$[*closo*-$B_{11}H_{11}$] and NCS in CH_2Cl_2.

Table S7. ^{1}H and ^{11}B NMR data of [*closo*-$B_{11}Cl_xH_{11-x}$]$^{2-}$ (x = 1–11), [*closo*-$B_{11}Cl_xBr_{11-x}$]$^{2-}$ (x = 6–10), and [*closo*-$B_{11}Cl_xI_{11-x}$]$^{2-}$ (x = 6–10) in CD_3CN.[a]

Anion	δ(^{11}B) (B–X[b]) [ppm]	δ(^{11}B) (B–Cl) [ppm]	δ(^{1}H) (B–H) [ppm]	^1J(^{11}B,^{1}H) [Hz]
[*closo*-$B_{11}H_{11}$]$^{2-}$	–16.7	–	1.08	129
[*closo*-$B_{11}ClH_{10}$]$^{2-}$	–17.3	–1.1	1.14	135
[*closo*-$B_{11}Cl_2H_9$]$^{2-}$	–17.8	–1.3	1.22	134
[*closo*-$B_{11}Cl_3H_8$]$^{2-}$	–18.5	–1.7	1.28	135
[*closo*-$B_{11}Cl_4H_7$]$^{2-}$	–19.2	–2.5	1.34	overlapped
[*closo*-$B_{11}Cl_5H_6$]$^{2-}$	–19.5	–3.6	1.40	overlapped
[*closo*-$B_{11}Cl_6H_5$]$^{2-}$	–19.6	–4.8	1.47	overlapped
[*closo*-$B_{11}Cl_7H_4$]$^{2-}$	–19.5	–5.9	1.55	140
[*closo*-$B_{11}Cl_8H_3$]$^{2-}$	–19.0	–6.8	1.66	overlapped
[*closo*-$B_{11}Cl_9H_2$]$^{2-}$	–18.1	–7.4	1.83	147
[*closo*-$B_{11}Cl_{10}H$]$^{2-}$	–16.6	–7.8	2.11	overlapped
[*closo*-$B_{11}Cl_{11}$]$^{2-}$	–	–6.1	–	–
[*closo*-$B_{11}Cl_6Br_5$]$^{2-}$	–9.0	–5.0	–	–
[*closo*-$B_{11}Cl_7Br_4$]$^{2-}$	–9.2	–5.3	–	–
[*closo*-$B_{11}Cl_8Br_3$]$^{2-}$	–9.4	–5.4	–	–
[*closo*-$B_{11}Cl_9Br_2$]$^{2-}$	–9.6	–5.6	–	–
[*closo*-$B_{11}Cl_{10}Br$]$^{2-}$	–9.8	–5.9	–	–
[*closo*-$B_{11}Cl_6I_5$]$^{2-}$	–17.4	–3.4	–	–
[*closo*-$B_{11}Cl_7I_4$]$^{2-}$	–17.8	–4.1	–	–
[*closo*-$B_{11}Cl_8I_3$]$^{2-}$	–18.2	–4.6	–	–
[*closo*-$B_{11}Cl_9I_2$]$^{2-}$	–18.6	–5.1	–	–
[*closo*-$B_{11}Cl_{10}I$]$^{2-}$	–19.0	–5.6	–	–

[a] [nBu$_4$N]$^+$ salts. [b] X = H, Br, I.

Crystal Structure Determination of $[nBu_4N]_2[closo\text{-}B_{10}Cl_{10}]\cdot CH_2Cl_2$ and $[nBu_4N]_2[closo\text{-}B_{11}Cl_xH_{11-x}]\cdot 0.5(CH_3)_2CO$ (x = 8 (50%), 9 (50%))

Colourless crystals of $[nBu_4N]_2[closo\text{-}B_{10}Cl_{10}]\cdot CH_2Cl_2$ and $[nBu_4N]_2[closo\text{-}B_{11}Cl_xH_{11-x}]\cdot 0.5(CH_3)_2CO$ (x = 8 (50%), 9 (50%)) were obtained from solutions in dichloromethane and acetone, respectively. Crystals were investigated with a Bruker X8-Apex II diffractometer using Mo-Kα radiation (λ = 0.71073 Å). All structures were solved either by direct (SHELXS)[14-15] or by intrinsic phasing methods (SHELXT).[14,16] Refinements are based on full-matrix least-squares calculations on F^2.[14,17] Calculations were performed with the ShelXle graphical interface.[18] Molecular structure diagrams were drawn with the program Diamond 4.5.1.[19] Experimental details, crystal data, and the CCDC numbers are collected in Table S8. These data can be obtained free of charge from The Cambridge Crystallographic Data Centre via www.ccdc.cam.ac.uk/data_request/cif.

$[nBu_4N]_2[closo\text{-}B_{10}Cl_{10}]\cdot CH_2Cl_2$: All non-hydrogen atoms were refined anisotropically. Most of the hydrogen atoms were located on a difference electron-density map. In the final steps of the refinement idealized bond lengths and angles were introduced for all H atoms. The solvate molecule is disordered over three positions and thus similarity and geometry restraints had to be applied to achieve a stable refinement.

$[nBu_4N]_2[closo\text{-}B_{11}Cl_xH_{11-x}]\cdot 0.5(CH_3)_2CO$ (x = 8 (50%), 9 (50%)): All non-hydrogen atoms were refined anisotropically. Most of the hydrogen atoms were located on a difference electron-density map. In the final steps of the refinement idealized bond lengths and angles were introduced for all H atoms. One butyl group of one of the four crystallographically independent $[nBu_4N]^+$ cations is disordered over three positions and the acetone solvate molecule is disordered over two positions. Each of the two independent $\{closo\text{-}B_{11}\}$ cluster reveals partial disorder as they represent a one to one mixture of the ions $[closo\text{-}B_{11}Cl_9H_2]^{2-}$ and $[closo\text{-}B_{11}Cl_8H_3]^{2-}$. In one case the isomers $[1,11\text{-}H_2\text{-}closo\text{-}B_{11}Cl_9]^{2-}$ and $[1,7,10\text{-}H_3\text{-}closo\text{-}B_{11}Cl_8]^{2-}$ are present and in the second case the isomers $[1,11\text{-}H_2\text{-}closo\text{-}B_{11}Cl_9]^{2-}$ and $[1,7,11\text{-}H_3\text{-}closo\text{-}B_{11}Cl_8]^{2-}$. The partial disorder of the anions, cations, and the solvent molecule required certain restraints to ensure a stable refinement.

Table S8. Selected Crystal Data and Details of the Refinement of the Crystal Structures of $[n\text{Bu}_4\text{N}]_2[closo\text{-B}_{10}\text{Cl}_{10}]\cdot\text{CH}_2\text{Cl}_2$ and $[n\text{Bu}_4\text{N}]_2[closo\text{-B}_{11}\text{Cl}_x\text{H}_{11-x}]\cdot0.5(\text{CH}_3)_2\text{CO}$ (x = 8 (50%), 9 (50%)).

	$[n\text{Bu}_4\text{N}]_2[closo\text{-B}_{10}\text{Cl}_{10}]\cdot\text{CH}_2\text{Cl}_2$	$[n\text{Bu}_4\text{N}]_2[closo\text{-B}_{11}\text{Cl}_x\text{H}_{11-x}]\cdot0.5(\text{CH}_3)_2\text{CO}$ (x = 8 (50%), 9 (50%))
Formula	$C_{33}H_{71}B_{10}Cl_{12}N_2$	$C_{67}H_{155}B_{22}Cl_{15}N_4O$
M_W	1029.41	1873.41
T (K)	100	100
Crystal system	triclinic	triclinic
Space group	P-1	P-1
a [Å]	12.4333(4)	12.1542(8)
b [Å]	12.6007(4)	20.4092(14)
c [Å]	19.7636(7)	23.6086(16)
α [°]	71.5730(10)	65.9960(10)
β [°]	75.3840(10)	76.1200(10)
γ [°]	73.4290(10)	77.1670(10)
volume [Å^3]	2770.42(16)	5142.2(6)
Z	2	2
ρ(calcd) [Mg m^{-3}]	1.234	1.210
μ [mm^{-1}]	0.626	0.492
F(000)	1074	1984
No. of collected reflections	39943	20483
No. of unique reflections	11776	12266
R(int)	0.0378	0.1422
No. of parameters/restraints	556 / 31	1106 / 74
$R1$ ($I > 2\sigma(I)$)	0.0704	0.0688
$wR2$ (all)	0.1506	0.1635
GOF on F^2	0.906	1.145
Largest diff. peak / hole / e Å^{-3}	1.521 / –1.384	1.538 / -1.080
CCDC no.	1819470	1819471

References

(1) Tozer, D. J.; Handy, N. C. Improving virtual Kohn–Sham orbitals and eigenvalues: Application to excitation energies and static polarizabilities. *J. Chem. Phys.* **1998**, *109*, 10180–10189.

(2) Häkkinen, H.; Yoon, B.; Landman, U. On the Electronic and Atomic Structures of Small Au_N^- (N = 4−14) Clusters: A Photoelectron Spectroscopy and Density-Functional Study. *J. Phys. Chem. A* **2003**, *107*, 6168–6175.

(3) Qin, Z.; Hou, G.-L.; Yang, Z.; Valiev, M.; Wang, X.-B. Negative ion photoelectron spectra of ISO_3^-, $IS_2O_3^-$, and $IS_2O_4^-$ intermediates formed in interfacial reactions of ozone and iodide/sulfite aqueous microdroplets. *J. Chem. Phys.* **2016**, *2016*, 214310.

(4) Warneke, J.; Hou, G.-L.; Aprà, E.; Jenne, C.; Yang, Z.; Qin, Z.; Kowalski, K.; Wang, X.-B.; Xantheas, S. S. Electronic Structure and Stability of $[B_{12}X_{12}]^{2-}$ (X = F−At): A Combined Photoelectron Spectroscopic and Theoretical Study. *J. Am. Chem. Soc.* **2017**, *139*, 14749–14756.

(5) Jenne, C.; Keßler, M.; Warneke, J. Protic Anions $[H(B_{12}X_{12})]$ (X = F, Cl, Br, I) That Act as Brønsted Acids in the Gas Phase. *Chem. Eur. J.* **2015**, *21*, 5887–5891.

(6) Volkov, O.; Paetzold, P.; Hu, C.; Kölle, U. Undecahalo-*closo*-undecaborates $[B_{11}Hal_{11}]^{2-}$. *Z. Anorg. Allg. Chem.* **2001**, *627*, 1029–1033.

(7) Boeré, R. T.; Derendorf, J.; Jenne, C.; Kacprzak, S.; Keßler, M.; Riebau, R.; Riedel, S.; Roemmele, T. L.; Rühle, M.; Scherer, H.; Vent-Schmidt, T.; Warneke, J.; Weber, S. On the Oxidation of the Three-Dimensional Aromatics $[B_{12}X_{12}]^{2-}$ (X = F, Cl, Br, I). *Chem. Eur. J.* **2014**, *20*, 4447–4459.

(8) Harris, R. K.; Becker, E. D.; Cabral de Menezes, S. M.; Goodfellow, R.; Granger, P. NMR Nomenclature. Nuclear Spin Properties and Conventions for Chemical Shifts. *Pure Appl. Chem.* **2001**, *73*, 1795–1818.

(9) Fulmer, G. R.; Miller, A. J. M.; Sherden, N. H.; Gottlieb, H. E.; Nudelman, A.; Stoltz, B. M.; Bercaw, J. E.; Goldberg, K. I. NMR Chemical Shifts of Trace Impurities: Common Laboratory Solvents, Organics, and Gases in Deuterated Solvents Relevant to the Organometallic Chemist. *Organometallics* **2010**, *29*, 2176–2179.

(10) Bernhardt, E.; Willner, H.; Verfahren zur Herstellung von *closo*-Boranaten. Bergische Universität Wuppertal, DE102008004530A1, 2009.

(11) Knoth, W. H.; Miller, H. C.; Sauer, J. C.; Balthis, J. H.; Chia, Y. T.; Muetterties, E. L. Chemistry of Boranes. IX. Halogenation of $B_{10}H_{10}^{-2}$ and $B_{12}H_{12}^{-2}$. *Inorg. Chem.* **1964**, *3*, 159–167.

(12) Tiritiris, I.; Schleid, T. Die Kristallstrukturen der Dicaesium-Dodekahalogeno-*closo*-Dodekaborate $Cs_2[B_{12}X_{12}]$ (X = Cl, Br, I) und ihrer Hydrate. *Z. Anorg. Allg. Chem.* **2004**, *630*, 1555–1563.

(13) Teeter, H. M.; Bell, E. W. *tert*-Butyl Hypochlorite. *Org. Synth.* **1952**, *32*, 20.

(14) Sheldrick, G. M. A Short History of SHELX. *Acta Crystallogr.* **2008**, *A64*, 112–122.

(15) Sheldrick, G. M. *SHELXS-97, Program for Crystal Structure Solution*; Universität Göttingen, 1997.

(16) Sheldrick, G. M. *SHELXT, Program for Crystal Structure Solution*; Universität Göttingen, 2014.

(17) Sheldrick, G. M. *SHELXL-97, Program for Crystal Structure Refinement*, Universität Göttingen, 1997.

(18) Hübschle, C. B.; Sheldrick, G. M.; Dittrich, B. ShelXle: A Qt Graphical User Interface for SHELXL. *J. Appl. Crystallogr.* **2011**, *44*, 1281–1284.

(19) Brandenburg, K. *Diamond 4.5.2*; Crystal Impact GbR, Bonn, Germany, 1997-2018.